Lateglacial–Holocene environments and human occupation in the Upper Lena region of Eastern Siberia derived from sedimentary and zooarchaeological data from Lake Ochaul

Franziska Kobe [a,*], Philipp Hoelzmann [b], Jana Gliwa [a,c], Pascal Olschewski [a,c], Sergey A. Peskov [d], Alexander A. Shchetnikov [e,f,g,h,i], Guzel A. Danukalova [j], Evgeniya M. Osipova [j], Tomasz Goslar [k,l], Christian Leipe [a,m], Mayke Wagner [c], Elena V. Bezrukova [e,f], Pavel E. Tarasov [a,**]

[a] Institute of Geological Sciences, Paleontology Section, Freie Universität Berlin, Malteserstraße 74–100, Building D, 12249 Berlin, Germany
[b] Institute of Geographical Sciences, Physical Geography, Freie Universität Berlin, Malteserstraße 74–100, Building B, 12249 Berlin, Germany
[c] Eurasia Department and Beijing Branch Office, German Archaeological Institute, Im Dol 2–6, 14195 Berlin, Germany
[d] Centre for the Preservation of Historical and Cultural Heritage of the Irkutsk Region, 5 Armii str. 2, Irkutsk 664025, Russia
[e] A.P. Vinogradov Institute of Geochemistry, Siberian Branch of the Russian Academy of Sciences, Favorskogo str. 1a, Irkutsk 664033, Russia
[f] Irkutsk Scientific Center, Siberian Branch of the Russian Academy of Sciences, Lermontova str. 134, Irkutsk 664033, Russia
[g] Institute of the Earth's Crust, Siberian Branch of the Russian Academy of Sciences, Lermontova str. 128, Irkutsk 664033, Russia
[h] Geological Institute, Russian Academy of Sciences, Pyzhevsky lane 7, Moscow 119017, Russia
[i] Laboratory of Geoarchaeology of Baikal Siberia, Irkutsk State University, 5 Armii str. 52, Irkutsk 664025, Russia
[j] Institute of Geology, Ufa Federal Research Centre of the Russian Academy of Sciences, Karl Marx str. 16/2, Ufa 450077, Russia
[k] Faculty of Physics, Adam Mickiewicz University, Umultowska 85, Poznan 61-614, Poland
[l] Poznan Radiocarbon Laboratory, Foundation of the Adam Mickiewicz University, Rubiez 46, Poznan 61-612, Poland
[m] Institute for Space-Earth Environmental Research (ISEE), Nagoya University, Furo-cho, Chikusa-ku, Nagoya 464-8601, Japan

ARTICLE INFO

ABSTRACT

In the current study, different geochemical and biological proxies, including pollen, non-pollen palynomorphs, ostracods and molluscs, from an AMS radiocarbon-dated sediment core from Lake Ochaul (54°14′N, 106°28′E; 641 m a.s.l.) are presented and discussed. Ochaul is a fresh-water lake and an archaeological site situated ca. 100 km northwest of Lake Baikal in the upper reaches of the Lena River. The 260-cm-long sedimentary record presented here spans the Lateglacial–Holocene interval, between ca. 13,500 cal yr BP and the present. The reconstructions of the postglacial vegetation and lake system development are discussed along with the regional climate dynamics and the hemispheric-scale environmental changes. During the Allerød interstadial the region around Lake Ochaul was dominated by sparse taiga forests. Cooling during the Younger Dryas led to a more open tundra landscape where trees formed patchy forest stands in climatically favourable environments. This facilitated a rapid spread of forests at the onset of the Early Holocene during which the study region was probably characterized by seasonally dry climate controlled by the interplay of higher insolation, lower global sea levels and remaining ice sheets in the North Atlantic region. After thermal and moisture optimum conditions and a maximum spread of forests during the Middle Holocene, continuous cooling and a trend to more open forests landscapes marked the Late Holocene. These long-term trends were interrupted by several relatively short episodes of change in the vegetation and algal records, which coincide with short-term (centennial-scale) Northern Hemisphere cooling/drying phases. This shows that the regional vegetation reacted sensitively to these climate oscillations. Six AMS radiocarbon dates of bone material of large herbivorous animals from the Ochaul archaeological site located at the northern shore of the lake provide important information about prehistoric hunter-gatherers and indicate that activities at the site took place at ca. 27,780–27,160 cal yr BP (95% probability range) as well as during the Mesolithic (ca. 8850–8450 cal yr BP), Early, Middle and Late Neolithic (between ca. 6840 and 5490 cal yr BP) and the Iron Age (ca. 2120–1930 cal yr BP). Our results demonstrate that

* Corresponding author.
** Corresponding author.
  E-mail addresses: FranziskaKobe@gmx.de (F. Kobe), ptarasov@zedat.fu-berlin (P.E. Tarasov).

despite major environmental transformations following the Last Glacial Maximum, Lake Ochaul and the Malaya Anga River valley remained attractive for large herbivores and for prehistoric hunter-gatherers, even during the Middle Neolithic cultural "hiatus" (ca. 6660–6060 cal yr BP) in Cis-Baikal, as documented by the published archaeological records.

1. Introduction

High-resolution pollen records preserved in lacustrine sediments remain the most common source of information on the postglacial vegetation and climate history and human-environment interactions in the vast regions of Northern Asia (e.g. Andreev et al., 2003; Bezrukova et al., 2010; Müller et al., 2010; Williams et al., 2011; Andreev and Tarasov, 2013; Binney et al., 2017). Involvement of other proxies, however, may provide more details and significantly improve robustness of the palaeoenvironmental reconstructions (e.g. Ashastina et al., 2018; Tarasov et al., 2019; Gromig et al., 2021).

The Baikal Archaeology Project (BAP) unites an international and multi-disciplinary team of scholars investigating hunter-gatherer culture dynamics in the Lake Baikal Region (LBR) of Siberia with a focus on the Middle Holocene interval between ca. 8300 and 3500 cal yr BP (Weber,

1995; Weber et al., 2002, 2010, 2013; Losey and Nomokonova, 2017). The new phase of the BAP (https://baikalproject.artsrn.ualberta.ca/), which began in 2018, aims at the reconstructions of individual life histories of Holocene hunter-gatherer culture dynamics using a comprehensive set of bioarchaeological and biogeochemical analytical methods, intensive AMS radiocarbon (^{14}C) dating, high-quality chronological control and detailed palaeoenvironmental records representing all geoarchaeological microregions (e.g. Kobe et al., 2020; Weber, 2020; Weber et al., 2021 and references therein). The main task of the palaeoenvironmental portion of this project (Tarasov et al., 2017) is to reconstruct the patterns of changes in past vegetation and climate in order to understand whether and in what way these changes could affect hunter-gatherers in the different parts of the LBR and to explain a well-documented lack of settlement and cemetery sites in the Cis-Baikal archaeological records during the Middle Neolithic, ca. 6660–6060 cal
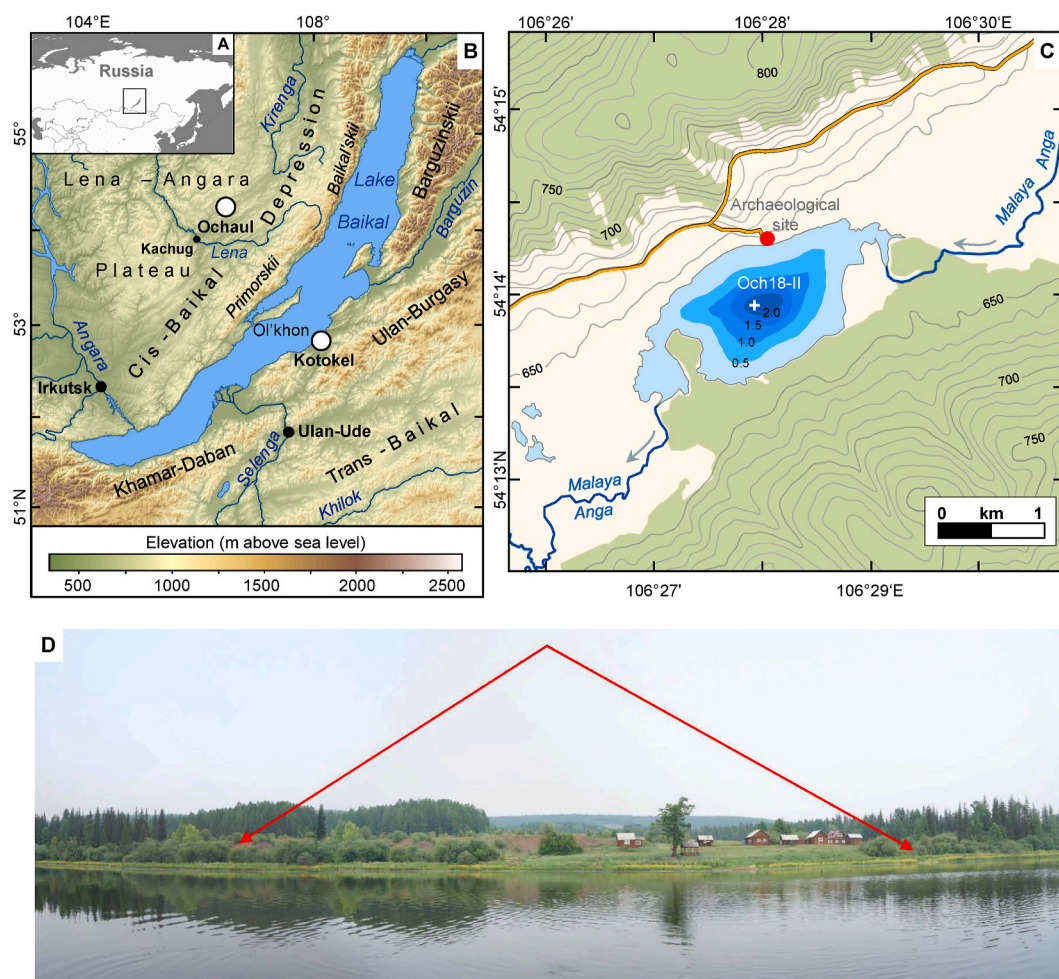

Fig. 1. (A) Overview map showing the location of the Lake Baikal Region (B) in northern Asia. (B) The topography and hydrology of the region around Lake Baikal in the southern part of Eastern Siberia with locations of the key pollen records from Lake Ochaul in Cis-Baikal and Lake Kotokel in the Trans-Baikal subregion. Locations of modern towns are provided for orientation. Topographic information is based on 90-m resolution Shuttle Radar Topography Mission (SRTM) v4.1 data (Jarvis et al., 2008). (C) Map of Lake Ochaul showing nearby environments and simplified bathymetry (after Kobe et al., 2021; after https://ru.mapy.cz/ with modifications) and the Och18-II core (white cross) and archaeological site (red point) locations. (D) Panoramic photo of the northern shore of Lake Ochaul (photo by S.A. Peskov, view from the southeast) with red arrows showing the western and eastern boundaries of the Ochaul archaeological site. The bathymetric survey was performed using a Humminbird HELIX 9 CHIRP GPS G4N echo sounder and chart plotter with a sonar frequency of 83/200/455 kHz. (For interpretation of the references to colour in this figure legend, the reader is referred to the Web version of this article.)

yr BP (Weber, 2020). The challenges in accomplishing this task and addressing these research questions remain low temporal resolution and poor dating control of most environmental records and their concentration in the coastal zone around Lake Baikal (Tarasov et al., 2017). In order to overcome these obstacles, high-resolution sedimentary archives representative of each archaeological microregion need to be found, robustly dated and analysed. Lake Ochaul in Cis-Baikal (Fig. 1) was suggested as a key site for geoarchaeological research in the Upper Lena microregion (Kobe et al., 2020). The 7.24-m-long core retrieved from the lake shows continuous sedimentation and spans the last 32,000 years (Kobe et al., 2021). Archaeological surveys conducted in the area also discovered a multi-layered archaeological site at the northern coast of Lake Ochaul (Aksyonov, 2009; Peskov, 2016) and suggested that the lake was visited by hunter-gatherers between the Mesolithic and the Bronze Age, although the existence of earlier Palaeolithic and later Iron Age camps was not entirely ruled out. The close proximity of an archaeological and environmental archive provides a key opportunity for in-depth multi-disciplinary geoarchaeological research at Lake Ochaul and offers great potential for studies of human-environmental interactions in the Upper Lena microregion of Cis-Baikal.

In order to test the potential of this environmental archive, Kobe et al. (2020) presented a coarse-resolution pollen analysis and a preliminary age model for the Lateglacial to Middle Holocene interval. The multi-century resolution of the first pollen record from Lake Ochaul was sufficient to discuss millennial-scale trends in vegetation development in Cis-Baikal prior to 4 cal kyr BP and for comparison with the Lake Kotokel pollen record from Trans-Baikal (Fig. 1A). However, the sensitivity of the Ochaul vegetation and the lake system to century-scale climate fluctuations and to Late Holocene cooling could not be tested. To fill this knowledge gap, the current study presents robustly dated results of a high-resolution palynological record of the Lake Ochaul sediment core Och18-II analysed at 2-cm steps, which covers the past 13,500 years including the Late Holocene. This record is supplemented by the results of geochemical, ostracod and mollusc analyses of the same core and zooarchaeological data (i.e. six AMS ^{14}C dates of bone fragments of large herbivores) obtained from cultural layers of a nearby archaeological site representing prehistoric hunter-gatherer camps. The newly obtained results are then used to discuss vegetation and climate dynamics, human-environment interaction history, and lake system evolution.

2. Environmental setting

The modern environments of the LBR are described in detail by Alpat'ev et al. (1976) and Galaziy (1993). Recently, Kobe et al. (2020) summarized the main features of the regional topography, hydrology, vegetation and climate, i.e. the factors that have played an important role in the lifestyle and subsistence strategies of human hunter-gatherers during the Late Pleistocene and Holocene periods. The LBR occupies about 1.2 million km^2 in the southern part of Siberia (Fig. 1A). The part of this huge region situated north and west of Lake Baikal (455 m a.s.l.) is called Cis-Baikal (in Russian *Pribaikalye*) and is characterized by a complex topography and hydrology (Fig. 1B), which affect local-scale climate and environmental variability. Boreal coniferous forests of various compositions, usually called 'taiga', occupy most of the region (Alpat'ev et al., 1976). However, 'tundra-like' vegetation associations are common in swampy areas, at lake shores and in river valleys (Kobe et al., 2020), and in the mountains above 1800 m (Bezrukova et al., 1996; Kozhova and Izmest'eva, 1998; Demske et al., 2005). Steppe-like associations frequently occur on east- and south-facing slopes across the entire region (Galaziy, 1993; Belov et al., 2002).

Lake Ochaul (54°14′N, 106°28′E; 641 m a.s.l.) is situated about 100 km northwest of Lake Baikal in the upper reaches of the Lena River (Fig. 1B). The Primorskii and Baikal'skii mountain ranges separate the lake catchment area from Lake Baikal, while the Lena-Angara Plateau borders it in the north and west (Kobe et al., 2021). Ochaul is a relatively small freshwater lake with a maximum length of ca. 2.7 km and a

maximum width of ca. 1.2 km (Boyarkin, 2007). The lake is rather shallow with a maximum water depth of about 2.5 m in its central part (Kobe et al., 2020). Water temperatures of about 0.7 and 14 °C and pH values of ca. 6.6 and 6.1 were measured in March and in June, respectively.

The lake is situated in a trough-shaped valley, a part of the large Cis-Baikal Depression, which stretches parallel to Baikal from the Angara River in the southwest to the Kirenga River in the northeast (Alpat'ev et al., 1976; Kobe et al., 2020). The valley has a flat and marshy bottom and slopes rising to 200–250 m above the lake level. It is drained by the Malaya Anga River – a tributary of the Bol'shaya Anga River, which flows into the Lena River near Kachug (Fig. 1B), a small town and county centre founded in 1686 (Kobe et al., 2021).

The bedrocks in the lake drainage area are represented by Middle–Upper Cambrian Verkholenskaya suite sedimentary rocks, including dolomite marls, mudstones, siltstones and sandstones with characteristic reddish-brownish colours (Vinogradov et al., 2011), which are transmitted in the process of lithogenesis to the overlying Cenozoic sediments (Kobe et al., 2021). The slopes of the valley around the lake are covered with boreal coniferous forest consisting of larch (*Larix* sp.), birch (*Betula* sect. *Albae* species) and Siberian pine (*Pinus sibirica*), with admixture of spruce (*Picea obovata*) and fir (*Abies sibirica*). The undergrowth is represented by shrubby birches (*Betula* sect. *Fruticosae* and *B.* sect. *Nanae*), shrubs of alder (*Alnus fruticosa*) and willow (*Salix*) and diverse members of the heath family (Ericaceae), including *Ledum palustre*, *Vaccinium vitis-idaea*, *V. uliginosum* as well as various herbaceous taxa, ferns and mosses (Kobe et al., 2020). Larch forests with abundant birch shrubs ('ernik') in the undergrowth also predominate in the lake catchment area (Belov et al., 2002).

The 30-year averages (1991–2020) from Kachug (53°58′12″N, 105°54′E, 521 m a.s.l.; http://www.pogodaiklimat.ru/history/30622.htm), ca. 50 km southwest of Lake Ochaul, provides an overview of the modern climate (Fig. 2). However, the precipitation and temperature values may vary significantly from year to year, i.e. between 216 and 466 mm (annual precipitation), between −35.8 and −19.1 °C (mean January temperature) and between +17 and +20.1 °C (mean July temperature), during the 1991–2020 interval.

The lake belongs to the 'Upper Lena archaeological microregion' of Cis-Baikal, rich in archaeological records of Palaeolithic, Mesolithic, Neolithic and Bronze Age hunter-gatherers (e.g. Zubkov, 2000; Weber et al., 2004; Aksyonov, 2009), though still remains understudied (Weber, 2020). Several archaeological surveys conducted around Lake Ochaul between 1913 and 2016 (Aksyonov, 2009; Peskov, 2016) discovered an archaeological site occupying a large area (Fig. 1D) on the northern shore of the lake (Fig. 1C).

3. Material and methods

3.1. Och18-II core lithology and chronological control

The 7.24-m-long sediment core Och18-II (54°13′58.4″N, 106°27′53.8″E) was recovered from 2.5 m water depth in the central part of Lake Ochaul in the summer of 2018. The coring was performed from a coring platform using a UWITEC percussion piston corer (Kobe et al., 2020).

The Och18-II core consists of water-rich soft organic gyttja (0–213 cm) rich in freshwater mollusc and ostracod shells (Fig. 3A), a transitional layer of gyttja and laminated silty clay (213–236 cm) and a thick layer of massive viscous silty clay (236–724 cm). The age-depth model of the Och18-II core based on 35 AMS dates has been presented and discussed in detail in Kobe et al. (2021) along with the results of the multi-proxy analysis of the Last Glacial Maximum interval. The age-depth model developed in Kobe et al. (2021) was applied to the records from the Lateglacial–Holocene part of the Och18-II core (0–260 cm) spanning the last ca. 13,500 years and the period discussed in the current study (Fig. 3B and Table 1).
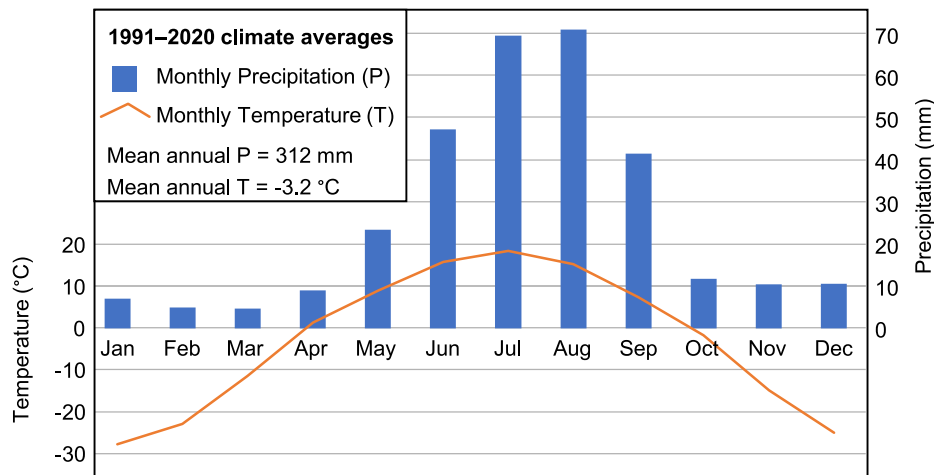
Fig. 2. Modern climate averages for the period 1991–2020 from the meteorological station at Kachug (http://www.pogodaiklimat.ru/history/30622.htm), ca. 50 km southwest of Lake Ochaul (Fig. 1B).
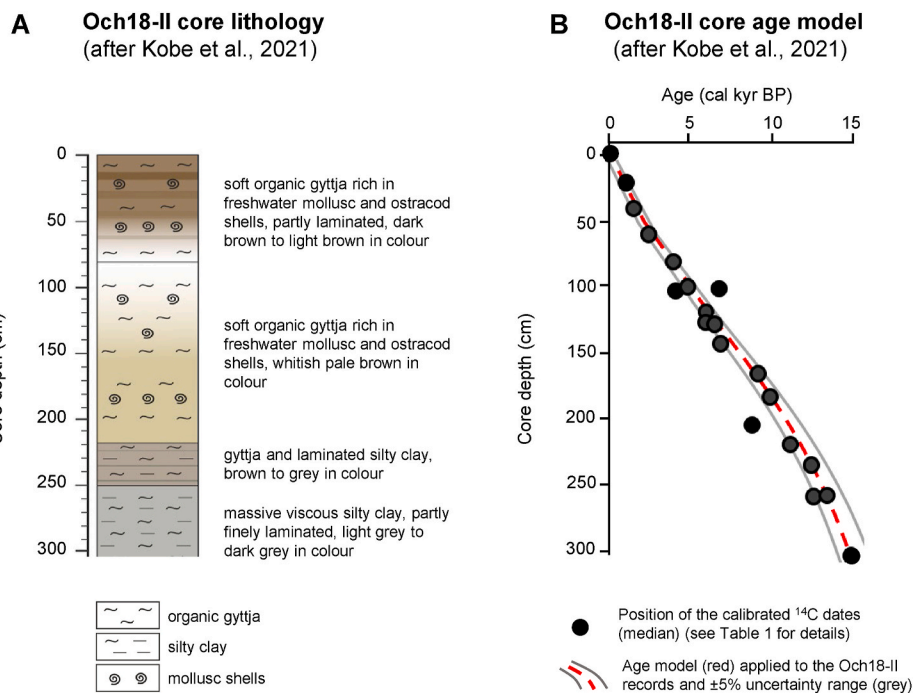

Fig. 3. (A) Simplified lithology and (B) age model of the studied section of the Och18-II sediment core (after Kobe et al., 2021).

3.2. Sediment properties

Physical and geochemical properties of the studied Och18-II core sediment section (Fig. 2A) were analysed at the Institute of Geographical Sciences (Berlin) and at the Institute of Geochemistry (Irkutsk), as described in Kobe et al. (2021). For grain-size measurements, chemical pre-treatment was done to isolate discrete particles of the sample from organic and carbonate cements and to provide an evenly dispersed suspension of individual particles (Sun et al., 2002). Organic matter was dissolved with a 10% solution of H_2O_2 (Allen and Thornley, 2004; Mikutta et al., 2005) and carbonate was eliminated by treatment with 10% HCl. The samples placed in test tubes were centrifuged for 15 min at a speed of 3000 rpm, then hydrogen peroxide and hydrochloric acid was removed, distilled water was added and the process was repeated. Finally, the samples were dried at 105 °C.

The core sediments were described visually in the laboratory. Biogenic silica (SiO_2bio) was measured at 1-cm intervals as described in

Mortlock and Froelich (1989). The sediment samples sampled at 1-cm steps were analysed for water content and dry bulk density (DBD) following a standard protocol (BDP-Members, 2004). The water content was measured immediately after the opening of the core. Specimens of about 1 cm^3 were weighed, dried at 60 °C and reweighed. DBD was measured by weighing sediment samples on a torsion balance in the air and in kerosene.

A standard set of geochemical analyses (Vogel et al., 2016), including elemental analysis of total carbon (TC), total inorganic carbon (TIC) and total organic carbon (TOC), as well as determination of sulphur by ICP-OES (inductively coupled plasma optical emission spectrometer) on the base of an aqua regia extraction (DIN EN, 2001) and portable energy-dispersive X-ray fluorescence spectrometry (P-ED XRF) with an Analyticon NITON XL3t of grinded and homogenised samples were conducted for all selected samples. The measurements were controlled with certified reference materials (LKSD-2 and LKSD-4; Lynch, 1990). As the elements Al, Ca, Fe, Rb, S, Si, and Zr show recovery values between

Table 1
Available AMS ^{14}C dating results (from Kobe et al., 2021) obtained on bulk sediment samples from the Lateglacial–Holocene section of the Och18-II sediment core (Fig. 2A) along with the respective calibrated ages (expressed as 95% probability ranges) and modelled median point estimates used in the age-depth model (Fig. 2B). All ^{14}C dates (in ^{14}C yr BP) were calibrated using OxCal v.4.4 software (Bronk Ramsey, 1995) and the IntCal20 calibration curve (Reimer et al., 2020).

Core segment ID	Radiocarbon laboratory number	Core composite depth, cm	Radiocarbon date, ^{14}C yr BP	Corrected radiocarbon date, ^{14}C yr BP	95% age range, cal yr BP	Modelled age, cal yr BP
Och18/II-1	Poz-106375	0–1	615 ± 30	15 ± 30	255–34	−47
Och18/II-1	Poz-114424	1–2	695 ± 30	95 ± 30	265–22	−6
Och18/II-1	Poz-114366	21–22	1855 ± 30	1255 ± 30	1280–1074	815
Och18/II-1	Poz-114367	41–42	2310 ± 30	1710 ± 30	1699–1535	1637
Och18/II-1	Poz-114409	61–62	3110 ± 30	2510 ± 30	2735–2490	2459
Och18/II-1	Poz-114410	81–82	4255 ± 35	3655 ± 35	4090–3877	3281
Och18/II-1	Poz-114411	101–102	4940 ± 30	4340 ± 30	5021–4844	4102
Och18/II-1	Poz-114412	127–128	5815 ± 30	5215 ± 30	6165–5910	6215
Och18/II-1	Poz-106373	129–130	6140 ± 40	5540 ± 40	6404–6280	6374
Och18/II-2	Poz-106374	100–101	6440 ± 40	5840 ± 40	6745–6502	4062
Och18/II-2	Poz-114413	104–105	4430 ± 30	3830 ± 30	4405–4101	4226
Och18/II-2	Poz-114415	124–125	5930 ± 35	5330 ± 35	6263–5996	5971
Och18/II-2	Poz-114416	144–145	6655 ± 35	6055 ± 35	6996–6797	7495
Och18/II-2	Poz-114417	164–165	8790 ± 50	8190 ± 50	9287–9015	8821
Och18/II-2	Poz-114571	184–185	9550 ± 50	8950 ± 50	10,225–9914	9994
Och18/II-2	Poz-114518	204–205	8630 ± 50	8030 ± 50	9031–8658	11,047
Och18/II-2	Poz-114419	218–219	10410 ± 50	9810 ± 50	11,317–11,166	11,724
Och18/II-2	Poz-114420	237–238	11070 ± 50	10470 ± 50	12,562–12,135	12,577
Och18/II-2	Poz-114421	258–259	12180 ± 50	11580 ± 50	13,540–13,291	13,443
Och18/II-2	Poz-106902	259–260	11340 ± 60	10740 ± 60	12,810–12,620	13,470

98 and 112% (Schwanghart et al., 2016) the values were not recalculated. The main mineralogic components were determined by XRD (X-ray diffraction: RIGAKU Miniflex600 at 15 mA/40 kV (Cu kα) from 3° to 80° (2θ) with a goniometer step velocity of 0.02° steps and 0.5° min^{-1}). The XRD-results are expressed in counts per second (cps), which reflects, semi-quantitatively, the proportion of the minerals.

3.3. Palynological analysis and pollen-based biome reconstruction

A total of 84 sediment samples (each representing a 1-cm depth interval) were taken in 2 to 4-cm steps from the upper 260-cm-long section of the Och-18-II core and treated for extraction of pollen, fern and moss spores and other non-pollen palynomorphs (NPPs) following the protocol described in Leipe et al. (2019). One tablet with exotic *Lycopodium* marker spores was added to each sample prior to chemical treatment in order to calculate the palynomorph concentrations (Stockmarr, 1971). All samples (each consisting of 1 g of sediment) were first treated with 10% HCl, to remove carbonates and to dissolve the calcareous matrix of the *Lycopodium* tablets, followed by a 10% KOH treatment in a hot water bath in order to remove humic acids. We used repeated low-speed centrifugation to remove fine silt and clay particles, followed by dense media separation using sodium polytungstate (SPT) heavy liquid at a density of 2.1 g/cm^3 to separate the pollen fraction from the remaining siliceous matter and other heavier particles. After SPT treatment and acetolysis, the sample residues were washed three times with distilled water and mounted in glycerol for microscopic analysis.

Pollen and non-pollen palynomorphs (NPPs) were counted using a light microscope at ×400 magnification and identified with the help of published atlases (van Geel, 1978, 2002; Reille, 1992, 1995, 1998; Jankovská and Komárek, 2000; Komárek and Jankovská, 2001; Beug, 2004; Demske et al., 2013; Savelieva et al., 2013) and the Section of Paleontology (FU Berlin) reference collection. Pollen produced by birch trees and birch shrubs was distinguished using morphological criteria discussed in Mäkelä (1996) and pollen of *Pinus* subgenus *Diploxylon* was distinguished from that of *P.* subgenus *Haploxylon* using morphological criteria discussed in Beug (2004) and Nakagawa et al. (2000). We aimed to count at least 400 terrestrial pollen grains per sample in order to reconstruct past vegetation composition without missing out on rare, but representative, taxa (e.g. Bennett and Willis, 2001).

Tilia version 1.7.16 software (Grimm, 2011) was used for calculating relative taxa percentages and for drawing the diagrams. Following Kobe et al. (2021), percentages for all terrestrial pollen taxa were calculated based on the sum of arboreal pollen (AP) and non-arboreal pollen (NAP) taken as 100%. Percentages for aquatic plants and terrestrial cryptogams were calculated based on the terrestrial pollen sum plus the sum of palynomorphs in the corresponding group. All NPPs are presented as absolute concentration values. The CONISS program for stratigraphically constrained cluster analysis by the method of incremental sum of squares (Grimm, 1987) was used to draw pollen zone boundaries.

Prentice et al. (1996) introduced a quantitative approach for the objective assignment of fossil pollen spectra to major vegetation types and for the robust comparison of the vegetation reconstruction results with the outcome of climate and vegetation modelling experiments. The reconstructed and simulated vegetation types or biomes are defined based on the ecological and bioclimatic characteristics and spatial distribution of pollen-producing plant taxa. The robustness of the biome reconstruction approach was tested using modern surface pollen data from northern Eurasia, including the LBR (Tarasov et al., 1998, 2005, 2013; Edwards et al., 2000; Müller et al., 2010; Binney et al., 2017). These successful tests of the method allowed its application for reconstructing the glacial-interglacial vegetation dynamics in the LBR over the past 500,000 years (Tarasov et al., 2005; Bezrukova et al., 2010; Prokopenko et al., 2010; Kobe et al., 2020, 2021). In the current study, we assigned all identified terrestrial pollen taxa to the corresponding regional biomes, following the biome-taxon matrix (Table 2) published in Kobe et al. (2020, 2021). Calculations of the biome affinity scores were performed using the equation published in Prentice et al. (1996), in which square root transformation was applied to pollen percentage values exceeding the universal threshold of 0.5% to increase the importance of minor pollen taxa. The biome with the highest affinity score or the one defined by a smaller number of contributing plant functional types and pollen taxa (when scores of several biomes are equal) was then assigned to each pollen spectrum (Prentice et al., 1996).

3.4. Other fossils: extraction and cleaning methods

In an attempt to obtain more biological proxies and to assess their potential for future high-resolution studies (e.g. stable isotope and trace element measurements) and environmental reconstructions, the Och18-II core sediments were first screened for calcareous fossils such as ostracods, molluscs and gyrogonites. It became clear that the sediment contains an unexpectedly rich variety of fossil taxa (Supplemental Fig.

Table 2

Terrestrial pollen taxa, exceeding the 0.5% universal threshold (Prentice et al., 1996), identified in the Late Quaternary pollen records from Northern Eurasia (Tarasov et al., 1998) and the Lake Baikal Region (Tarasov et al., 2009a; Bezrukova et al., 2010; Müller et al., 2014; Kobe et al., 2020, 2021) and their assignments to the respective biomes. Taxa indicated with an asterisk do not exceed 0.5% in the analysed Och18-II core samples and therefore did not influence biome score calculations.

Biome name	Taxa included
Tundra	*Alnus fruticosa, Betula* sect. *Nanae, Salix*, Ericales*, Cyperaceae, Poaceae, *Polemonium*, Polygonaceae*, Saxifragaceae*, Scrophulariaceae*, Valeriana*
Cold deciduous forest	*Pinus* (subgen. *Diploxylon*-type), *Pinus* (subgen. *Haploxylon*-type), *Larix, Alnus* (tree)*, *Betula* sect. *Albae*, Ericales*, *Salix*,
Taiga	*Abies, Picea, Pinus* (subgen. *Diploxylon*-type), *Pinus* (subgen. *Haploxylon*-type), *Larix, Alnus* (tree)*, *Betula* sect. *Albae*, *Corylus*, Ericales*, Ribes*, Salix*
Cool conifer forest	*Abies, Picea, Pinus* (subgen. *Diploxylon*-type), *Pinus* (subgen. *Haploxylon*-type), *Larix, Alnus* (tree)*, *Betula* sect. *Albae*, *Corylus*, Ulmus*, Ericales*, Ribes*, Salix*
Steppe	Apiaceae*, *Artemisia*, Asteraceae (Asteroideae), Asteraceae (Cichorioideae), Brassicaceae, Cannabaceae, Caryophyllaceae*, Chenopodiaceae, *Epilobium*, Fabaceae*, Lamiaceae*, Liliaceae*, *Allium*, Plantago*, *Poaceae, Polygonaceae*, Ranunculaceae, *Thalictrum*, Rosaceae, Rubiaceae, Scrophulariaceae*, *Urtica*, Valeriana*
Desert	*Artemisia*, Boraginaceae*, Chenopodiaceae, *Ephedra*, Polygonaceae*

S1). The small sediment subsample size (i.e. 2–6 g) prevented the use of standard preparation techniques (e.g. decalcification or alkaline solutions) developed for single fossil groups. Other challenges resulted from the different geochemical properties of the sediment, the mix of the contained calcareous, apatite, siliceous, chitinous and organic plant microfossils and the high content of organic material.

For the determination of an optimal extraction and cleaning method, 5 samples (2–6 g each) were divided in 12 subsamples and treated with the following common microfossil preparation methods: 1) ultrasonic bath, 2) potassium hydroxide, 3) Rewoquat® and 4) hydrogen peroxide. In a first attempt to disintegrate the sediment mechanically an ultrasonic bath was used for 1–10 min as suggested by Wissing and Herrig (1999). The fossil material (sediment and single ostracod valves) was put in a ceramic bowl with water and placed in the ultrasonic bath and examined afterwards. However, as the shell material and especially ostracod valves were damaged, the ultrasonic treatment was rejected.

Potassium hydroxide (KOH) is commonly used to deflocculate organic rich samples (Bates et al., 1978). Our test samples were treated with 5% and 10% KOH for a duration of 1–24 h. No effect on the sediment matrix was observed, possibly due to the high content of calcareous material. Rewoquat® has been reported as very efficient for disintegrating clayey sediment samples and cleaning fossils (Wissing and Herrig, 1999). It was used in a pure state and diluted with ethanol, following the descriptions in Wissing and Herrig (1999) and Jarochowska et al. (2013), however, without any noticeable disintegrative effect. The sediment soaked with Rewoquat® mixed with ethanol did not interact with watery solutions afterwards, making any further handling extremely difficult.

The best results were achieved using a low concentration of hydrogen peroxide (H_2O_2), which is considered one of the least harmful chemicals for the purpose of cleaning ostracods in these studies (Keatings et al., 2006; Li et al., 2007). It was found that the Lake Ochaul sediment samples react quite differently depending on composition. While samples rich in organic and calcareous material may require a 24-h treatment with 10% H_2O_2, samples comprising mainly terrigenous siliciclastic material became sufficiently loose already after 2 h of treatment with 5% H_2O_2. Here, an approach was chosen to treat the samples with 5 or 10% H_2O_2 as long as necessary, but as short as possible. The following steps were employed.

1) The sediment sample was weighed and rinsed with tap water using a sieve with a 106 μm mesh size. The fraction larger than 106 μm was placed in a plastic container and put in a freeze drier (ca. −60 °C) for 7–16 h depending on sample size. During rinsing, the excess water was collected in a 5-L beaker, allowing time for the sediment particles smaller than 106 μm to settle. In most cases, sufficient sediment settled from suspension after 5–10 min. Investigations of this residue showed that it contained abundant sponge spicules, remains of algae, testate amoebae and other fossils. Pollen and NPPs of a similar size were rarely found. The sediment <106 μm was dried in a heating oven at 40 °C overnight.

2) After drying, the small fraction was stored in plastic containers. The fraction >106 μm was examined for chitinous fossils, plant debris, molluscs, if the periostracum was preserved, and larger clean objects, such as fish teeth. If needed, these fossils were cleaned manually with a brush and water. The remaining sediment, which still forms coherent lumps was treated with H_2O_2. To estimate the necessary reaction time, a small amount of every sample was tested using 5% H_2O_2. This prevents over-treatment and possible damage of the fossils and saves time. As under-treatment of the organic rich samples can result in a thin coating of organic matter on the fossils, the samples rich in organic matter should be treated with 10% H_2O_2.

3) Following the results of the test, the samples were treated with 5 or 10% H_2O_2 usually for 2, 4, 5, 7 or 24 h. Longer treatment requires regular checks to avoid any negative effects. The samples are then rinsed again as described above. Then, the fraction <106 μm can be oven-dried and the fraction >106 μm must be freeze-dried. In optimal cases, fossils were free of sediment and ready for subsequent picking with a fine brush or needle after freeze-drying.

3.5. Ostracod analysis

For the analysis of ostracods, 41 sediment samples, each representing a 1-cm-thick slice, have been taken from the analysed core section. The samples were treated according to the protocol described in section 3.4. and in Kobe et al. (2021). For species identification, ostracods from 34 sediment samples with a high ostracod concentration were sputtered with gold and photographed using a Leica S430 Scanning Electron Microscope (SEM) at the German Archaeological Institute, Berlin and a ZEISS SUPRA™ 40 V P Ultra SEM at the FU Berlin. Species were identified with the ostracod determination keys published by Meisch (2000) and Fuhrmann (2012) and species descriptions in Bronstein (1947) and Mazepova (1990). Species richness was calculated for all samples with identified species.

3.6. Malacological analysis

Shells of land and freshwater molluscs can be abundant in a range of Quaternary sediments and several recent studies of terrestrial geological sections in the LBR demonstrated the significance of well-dated molluscan successions for the reconstruction of Late Pleistocene and Holocene palaeoenvironments (e.g. White et al., 2008; Danukalova et al., 2015; Shchetnikov et al., 2019). In this study, mollusc shells were extracted from the Och18-II core sediment samples selected for the ostracod analysis in order to test the potential of malacological analysis for further in-depth research. In total, 5 samples were selected, which represent the 25–26 (ca. 980 cal yr BP), 33–34 (ca. 1310 cal yr BP), 133–134 (ca. 6530 cal yr BP), 196–197 (ca. 10,640 cal yr BP) and 229–230 cm (ca. 12,230 cal yr BP) levels and the most characteristic intervals in the palynological and sedimentary records.

A single bivalve shell was counted if more than 50% of the shell were preserved (Foster et al., 2018). Taxonomic identification was done using the descriptions and published reference keys of Zhadin (1952), Nederlandse Fauna 2 (1998), Falkner et al. (2002), Glöer (2002, 2019), Sanko (2007), Welter-Schultes (2012), Rogers (2019) and Khokhutkin et al. (2009) for Lymnaeidae. Each specimen was identified to the level

of genus and, if possible, species. A precise taxonomic evaluation and re-assessment of the gastropod genus *Gyraulus* has yet to be achieved (*sensu* Glöer, 2002; Rogers, 2019). In Rogers (2019), *G. rossmaessleri* (Auerswald, 1852) is described as *Lamorbis rossmaessleri* and *G. crista* (Linnaeus, 1758) as *Armiger crista*. The possible synonym "*Armiger crista*" is also often used for *G. crista* (e.g. Richardot-Coulet and Alfaro-Tejera, 1985). Here, the concept of Glöer (2002, 2019) is accepted, according to which *Lamorbis* Starobogatov, 1967 and *Armiger* Hartmann, 1843 may represent subgenera of the genus *Gyraulus* Charpentier, 1837.

3.7. Zooarchaeological material from the Ochaul site

The cultural layers of the archaeological site at the northern shore of Lake Ochaul (Fig. 1C and D) are confined to the terrace and alluvial cone surfaces elevated up to 1.5–10 m above the modern lake level. The Ochaul site was first discovered by B.E. Petri in 1913. In 1971, it was visited by the archaeological team of the Complex Archaeological Expedition, Irkutsk State University (ISU), led by M.P. Aksyonov, who organised the first surface survey.

In 1989, the site was revisited and studied by the Upper Lena Research Team of the Middle-Siberian Archaeological Expedition, ISU, supervised by V.M. Vetrov, N.E. Berdnikova and N.A. Saveliev. They performed topographic and photographic surveys of the site, collected surface material and investigated several test pits at the alluvial fan. Cultural remains were recorded between 3 and 16 m above the lake level and in the blackish humified sandy loam layer up to a depth of 0.40 m from the modern surface. The archaeological finds were typologically assigned to the Mesolithic and Neolithic period and dated back to ca. 8000–5000 years ago. In 1995, a part of the archaeological site was destroyed during the construction of a reservoir for sapropel, the area of destruction was 100 × 200 m. In 2001, S.N. Perzhakov carried out monitoring and estimated the total area of the archaeological site to be about 120,000 m².

In 2016, archaeological work was carried out by S.A. Peskov and S.N. Perzhakov, who excavated and investigated cultural layers in six test pits, named pits No. 1 (2 × 2 m), No. 2 (1 × 2 m) and No. 3–6 (2 × 2 m). In the course of the trial excavations and surface surveys, rich archaeological material was discovered, including tools and weapons made of stone and elk bone, shards of ornamented and plain ceramic vessels, animal bone fragments and scattered human remains. The scattered human bones also suggest burial activities at the site sometime in the past, although no graves have yet been found. The cultural layers were typologically and tentatively assigned to the relatively broad time interval from the Mesolithic to the Bronze Age, albeit an occupation in the Late Pleistocene was also considered after a bone fragment of an extinct wild horse was excavated. For this study, six bone fragments of wild ungulate species (all showing traces of anthropogenic modifications) from the archaeological collections of 1989 (cultural layer 35–55 cm below surface) and 2016 (cultural layer 30–75 cm below surface) were selected (Table 3) and sent to the Poznan Radiocarbon Laboratory for AMS ¹⁴C age determination. All bioarchaeological dates were converted to calendar ages using OxCal v4.4 (Bronk Ramsey, 1995) and the

IntCal20 curve (Reimer et al., 2020).

4. Results

4.1. Sediment properties

The results of the physical and geochemical analyses of the Och18-II sediment are summarized in Fig. 4 and Supplemental Fig. S2. The section is composed of organic gyttja and silty clay. Its main characteristics are relatively high TOC (5.6–28.4%) and TIC. Calcite ($CaCO_3$) is the main mineral, except during the Lateglacial (ca. 13,500–11,650 cal yr BP) and during the last 1200 years when quartz (SiO_2) dominates. Pyrite (FeS_2) is present throughout the entire section and is highest when Ca contents are low during the Lateglacial and the last 2200 years. The composition of the remaining minerals is similar to that of the Last Glacial Maximum sequence (LGM; Kobe et al., 2021) with phyllosilicates (muscovite $[KAl_2(Si_3Al)O_{10}(OH)_2]$ and chlorite $[MgxAlxCrxAlx-Six_4-O_{10}(O)_8])$ and silicates (albite $[Na(AlSi_3O_8)]$ as feldspar). Biogenic silica (SiO_2bio) shows higher contents (up to 3%) in the uppermost part of the core (4200 cal yr BP to present). Based on sediment properties, the entire core has been divided into four main sediment zones (SZ-1 to 4) (Fig. 4).

SZ-1 (260–217 cm; ca. 13,500–11,650 cal yr BP) consists of silty clay and is characterised by changes in the mineralogic contents of calcite, quartz and pyrite. Consequently, the concentrations of Ca, Ti, Fe, S, P and organic and inorganic carbon also exhibit changing values. This interval can be divided into two subzones SZ-1a (260–240 cm; 13,500–12,660 cal yr BP) and SZ-1b (240–217 cm; 12,660–11,650 cal yr BP).

SZ-2 (217–150 cm; ca. 11,650–8000 cal yr BP) consists of organic gyttja and shows minor changes in its main components such as calcite, quartz and pyrite and relatively stable values for nearly all other parameters, such as Ca, Ti, Fe, S, and P. Organic and inorganic carbon show constantly high values and only minor changes throughout this interval.

SZ-3 (150–60 cm; ca. 8000–2200 cal yr BP) is very similar to SZ-2, but the organic gyttja in the lower part (SZ-3a: 150–104 cm; ca. 8000–4260 cal yr BP) exhibits slightly lower organic carbon contents and minimal fluctuations in the other components.

SZ-4 (60 cm to top of core Och18-II; 2200 cal yr BP to the coring year 2018) composed of organic gyttja is characterized by changing sediment parameters and the highest organic carbon contents. The calcite content decreases towards the top of the core whereas quartz, biogenic silica and, in particular, pyrite show increasing values (Fig. 4).

4.2. Palynological assemblages and reconstructed biomes

The results of the pollen analysis and pollen-based biome reconstruction are summarized in Fig. 5, while the aquatic pollen, fern spores and other NPP taxa are shown in Fig. 6. The entire record has been divided into nine local pollen zones called PZ-1 to 9.

PZ-1 (260–240 cm, ca. 13,500–12,660 cal yr BP) is characterized by moderately high tree (up to 61.5%) and shrub (up to 18%) percentages

Table 3
Available ¹⁴C dating results from the archaeological site Ochaul (this study) discussed in the current paper. The ¹⁴C dates (in ¹⁴C yr BP) were calibrated using OxCal v.4.4 software (Bronk Ramsey, 1995) and the IntCal20 calibration curve (Reimer et al., 2020). Calibrated ages are expressed as 95% probability ranges.

| Zooarchaeological sample number	Laboratory code	Dated bone material	¹⁴C date (¹⁴C yr BP)	Calibrated age, 95.4% range (cal yr BP)	Laboratory remark
1989 collection					
Och-1989-2	Poz-134277	*Capreolus* sp.	2070 ± 35	2124–1930	1.4% N, 7.9% C, 5.5% collagen
Och-1989-1	Poz-134275	*Capreolus* sp.	4855 ± 35	5716–5489	1.9% N, 8.6% C, 5% collagen
2016 collection					
Och-2016-2	Poz-134279	*Alces* sp.	5595 ± 50	6487–6296	1.3% N, 7.3% C, 3.9% collagen
Och-2016-3	Poz-134280	Cervidae sp.	5870 ± 50	6837–6507	2.0% N, 8.2% C, 5.3% collagen
Och-2016-1	Poz-134278	*Capreolus* sp.	7820 ± 50	8851–8449	2.8% N, 9.9% C, 5.5% collagen
Och-2016-4	Poz-134281	*Equus* sp.	23170 ± 220	27785–27158	3.2% N, 10.9% C, 7.8% collagen
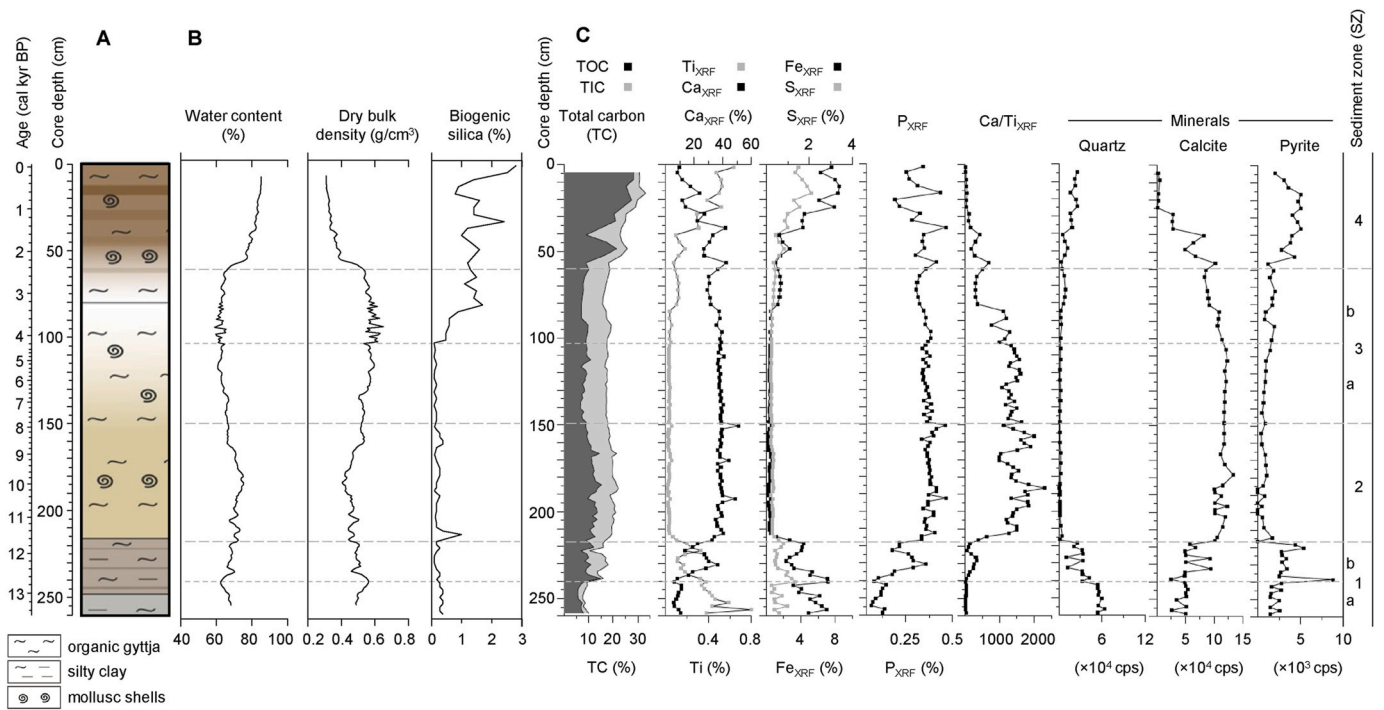
Fig. 4. Selected sediment properties (B) and geochemical parameters (C) of the studied section of the Och18-II sediment core (A).
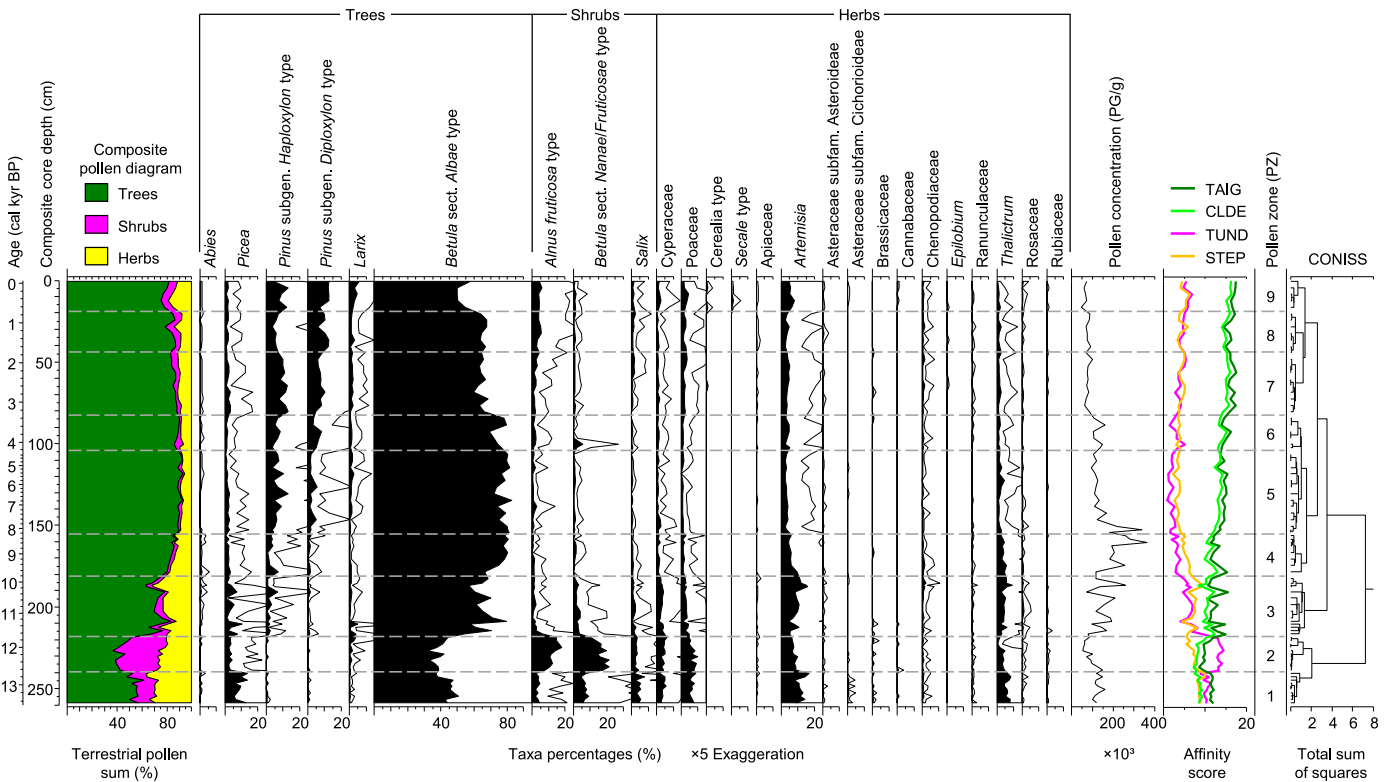

Fig. 5. Simplified percentage diagram showing results of pollen analysis and calculated affinity scores of the major regional biomes: taiga (TAIG), cold deciduous forest (CLDE), tundra (TUND) and cool steppe (STEP).

mainly represented by *Betula* sect. *Albae* (37–50%), *Picea* (5–14%), *Alnus fruticosa* (2–5%), *Betula* sect. *Nanae/Fruticosae* (4–9%) and *Salix* (1–8%). The NAP contribution (up to 36%) is relatively high, especially for *Artemisia* (8–17%), Cyperaceae (2–6%), Poaceae (5–9%) and *Thalictrum* (4–8%). The biome reconstruction shows the highest scores for the taiga

(TAIG) biome, closely followed by tundra (TUND). Among the NPP taxa, green algae *Botryococcus* and *Pediastrum* show very high concentrations, with a dominance of *P. boryanum* (up to 980,000 coenobia/g) followed by *P. kawraiskyi* and *P. duplex*.

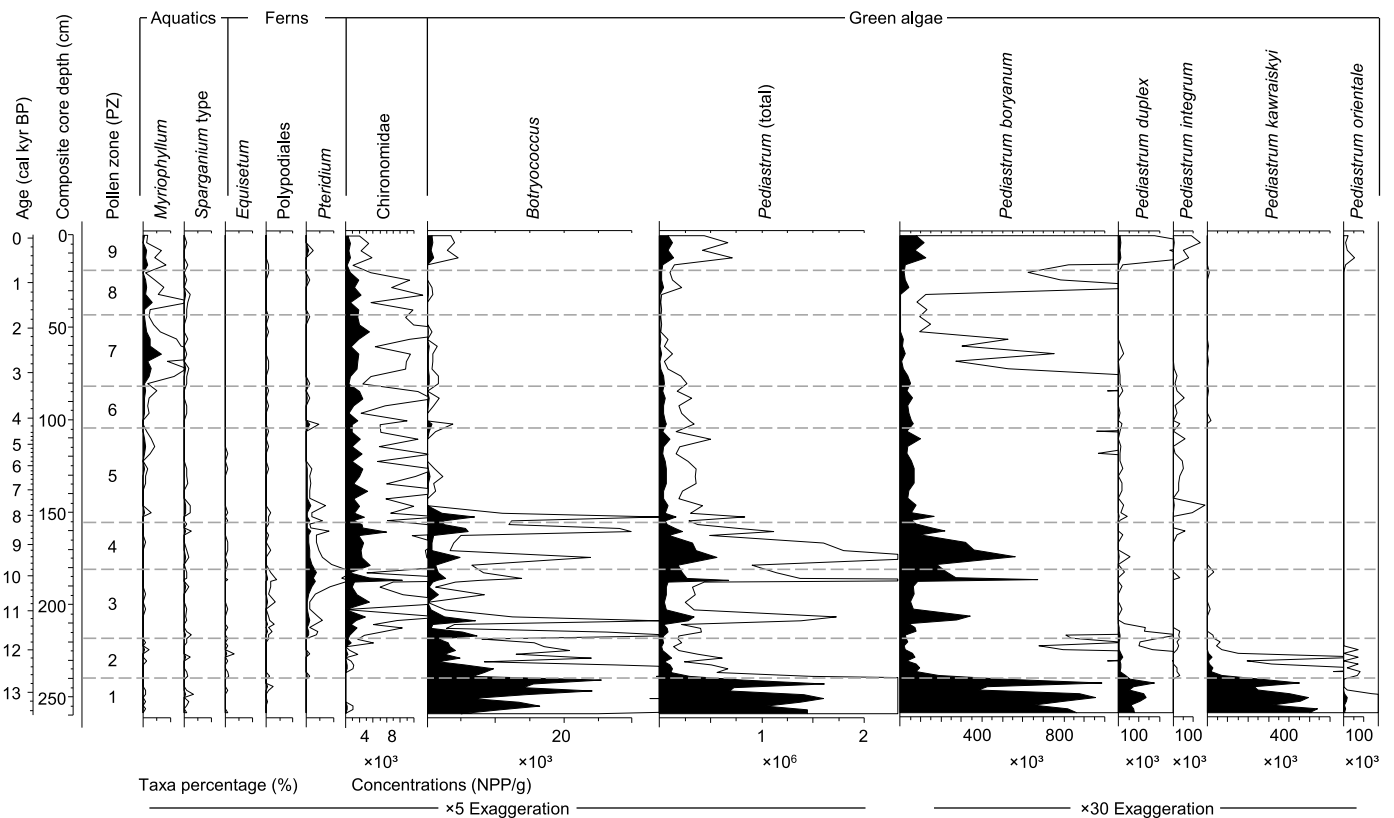PZ-2 (240–218 cm, 12,660–11,680 cal yr BP) reveals the highest

Fig. 6. Simplified diagram showing aquatic pollen and fern spore percentages and absolute concentrations of counted chironomid and green algae remains.

percentages for boreal shrubs (up to 37.5%), lowest percentages for trees (39–45%) and moderately high NAP percentages (up to 28%). The tundra biome has the highest score. Algae concentrations decrease rapidly, especially for *Pediastrum*. The concentrations of *Botryococcus* and *P. kawraiskyi* show a constant decreasing trend towards the upper zone boundary. *P. integrum* (up to 1000 coenobia/g) and *P. orientale* (up to 2500 coenobia/g) appear in this PZ.

PZ-3 (218–181 cm, 11,680–9770 cal yr BP) shows a decrease in shrub taxa percentages (down to 12%), dominance of *B.* sect. *Albae* (54–80%), increasing values of coniferous taxa like *Abies* (up to 1%), *Picea* (0,5–10%), *Pinus* (*Haploxylon* type up to 7% and *Diploxylon* type up to 1.5%) and *Larix* (up to 5%). The taiga biome scores are the highest again. Polypodiales (up to 1%) and *Pteridium* (up to 3.5%) fern spores show slightly higher values. Concentrations of green algae remain generally low, although *P. boryanum* shows two distinct peaks.

PZ-4 (181–155 cm, 9770–8250 cal yr BP) shows high AP values (up to 89%) and the dominance of *B.* sect. *Albae* (66–81%). The NAP percentages decrease from 17.5 to 11%, which is also visible in decreasing scores of the cool steppe (STEP) and tundra biomes.

PZ-5 (155–104 cm, 8250–4260 cal yr BP) demonstrates the highest AP values (up to 94.5%), accompanied by the higher percentages of *P.* subgen. *Haploxylon* (3.5–13%), *P.* subgen. *Diploxylon* (1–5.5%) and *Larix* (up to 3%). The taiga biome keeps its dominant role. Pollen of aquatic *Myriophyllum* (up to 1%) appears in growing numbers. Algae concentrations are low and *Botryococcus* even disappears at several levels. *Pediastrum* concentrations remain stable. *P. boryanum* dominates with *P. duplex* and *P. integrum* being present.

PZ-6 (104–83 cm, 4260–3320 cal yr BP) shows a drop in *B.* sect. *Albae* percentages to 69.5% in the middle of the zone and an increase in *P.* subgen. *Diploxylon* to 8.5%. Percentages of shrubby taxa increase slightly (1.5–7.5%) and a small peak of *B.* sect. *Nanae/Fruticosae* (5.5%) is registered at 100 cm (about 4060 cal yr BP). No changes appear in the algae record.

PZ-7 (83–46 cm, 3320–1840 cal yr BP) reveals a continuous decrease in AP from 88 to 84% and a parallel increase in shrub pollen from 2.5 to 5%. The relative contribution of coniferous taxa also increases. NAP percentages increase to 8–11%. Single occurrences of *Epilobium* are registered in this and in the two uppermost zones. *Myriophyllum* percentages increase to 6.5%. Green algae almost disappear towards the upper zone boundary.

PZ-8 (46–19 cm, 1840–690 cal yr BP) shows a similar composition to the previous zone with a minor decrease in *Picea* to 2% and *P.* subgen. *Haploxylon* (3.5–7%) and an increase of *P.* subgen. *Diploxylon* (6–12.5%). Percentages of *A. fruticosa* shrubs show a clear increase to 5.5%. Noteworthy is the temporary drop in AP to 86% at 28 cm (1100 cal yr BP). Pollen percentages of *Myriophyllum* are still moderately high (up to 3.5%). Concentrations of green algae are still low, but show an increase towards the upper zone boundary.

PZ-9 (19–0 cm, 690 cal yr BP onwards) is characterized by slightly lower AP percentages. *B.* sect. *Albae* values decrease to 50% in the middle of the zone, although all coniferous taxa show slight increases in abundance. Poaceae (up to 4%) and *Artemisia* (up to 8%) occur more frequently. These changes coincide with the presence of Cerealia-type, *Secale* (up to 0.7% each) and Cannabaceae pollen. Although biome scores of tundra and steppe increase throughout the zone, taiga remains the dominant biome. Concentrations of green algae increase once again in this zone. *P. boryanum* dominates but *P. duplex*, *P. integrum*, *P. orientale* and *Botryococcus* are registered as well.

4.3. Ostracods

In total, 39 of 41 analysed samples contained ostracods. In these samples, the amount of ostracod valves ranged from a few to approximately 1000 specimens per sample (Fig. 7). Especially the lower 20-cm and upper 26-cm intervals are characterized by very low ostracod occurrences of a maximum of 8 valves per sample. Most of the remaining
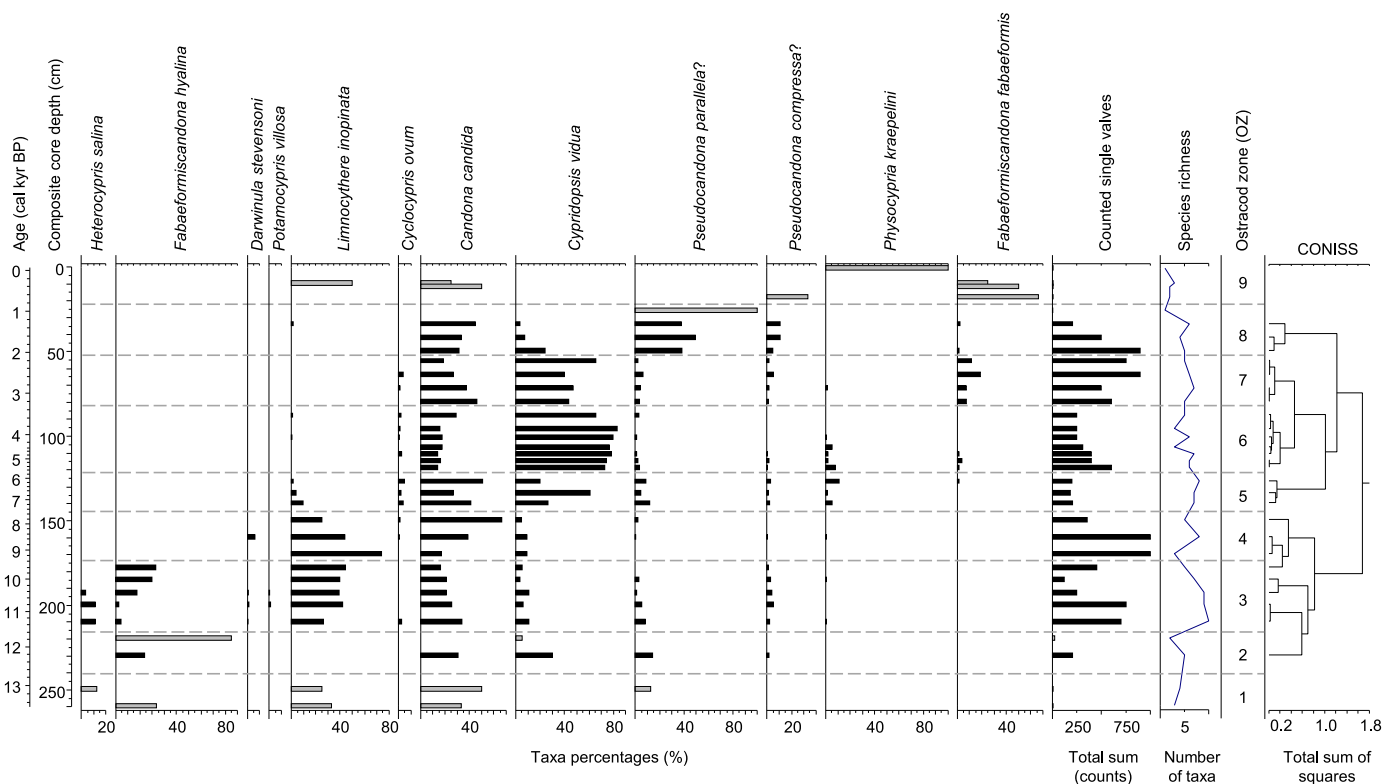
Fig. 7. Percentage diagram showing results of ostracod analysis.

samples (except one sample) yielded more than 100 single ostracod valves each.

In total, 3940 ostracod valves from the selected sediment samples were identified to species level (Fig. 7). In the investigated core segment, we found an ostracod fauna comprising the following 12 species (Fig. 8): *Candona candida* (O.F. Müller, 1776), *Pseudocandona parallela*? (G.W. Müller, 1900), *Limnocythere inopinata* (Baird, 1843), *Heterocypris salina* (Brady, 1868), *Fabaeformiscandona hyalina* (Brady and Robertson, 1870), *Cypridopsis vidua* (O.F. Müller, 1776), *Darwinula stevensoni* (Brady and Robertson, 1870), *Cyclocypris ovum* (Jurine, 1820), *Physocypria kraepelini* (G.W. Müller, 1903), *Pseudocandona compressa*? (Koch, 1838), *Potamocypris villosa* (Jurine, 1820) and *Fabaeformiscandona fabaeformis* (Fischer, 1851). With the help of CONISS, the ostracod record was divided into nine ostracod zones further called OZ-1 to 9 (Fig. 7).

OZ-1 (260–239 cm, ca. 13,500–12,650 cal yr BP) consists of two productive samples from 249 to 250 and 259–260 cm with a very low ostracod content (4–8 valves). Their relative species occurrences are therefore not representative for the ancient ostracod community. Five different species could be distinguished (*C. candida, P. parallela*?, *L. inopinata, H. salina* and *F. hyalina*).

OZ-2 (239–217 cm, ca. 12,650–11,650 cal yr BP) also consists of two productive samples, while the lowest sample (239–240 cm) was free of ostracods. The assemblage is dominated by *C. candida* and *C. vidua* (30% each) and *F. hyalina* (24%). The sample from 219 to 220 cm comprises only 19 valves and is dominated by *F. hyalina* (95%).

OZ-3 (217–173 cm, ca. 11,650–9330 cal yr BP) is characterized by the appearance of *H. salina* (up to 12%) and an increasing relative abundance of *F. hyalina* (up to 33%), which both disappear in the core sediment above. *L. inopinata* (26–44%) and *C. candida* (16–34%) are co-dominant and *D. stevensoni, C. vidua, P. parallela, C. ovum, P. kraepelini, P. compressa* and *P. villosa* are present in this zone. With up to 10 species per sample, this zone shows the highest diversity of the investigated core section; the absolute numbers of ostracod valves are relatively high.

OZ-4 (173–145 cm, ca. 9330–7530 cal yr BP) is co-dominated by *L. inopinata* (max. 74%) and *C. candida* (max. 67%). *D. stevensoni* reaches

its maximum (7%) before it disappears from the record. The absolute numbers of ostracod valves are highest (up to 1000 specimens per sample) in this zone.

The following three zones (OZ-5 to OZ-7; 145–52 cm, ca. 7530–2070 cal yr BP) show some similarities in assemblage composition, but noticeable differences in the percentages of contributing taxa. The main feature is a change in the ostracod composition from *L. inopinata*-dominated to *C. vidua*-dominated (up to 79%) assemblages with only a few occurrences of *L. inopinata*. The ostracod assemblages of OZ-5 are characterized by high occurrences of *C. candida* (up to 51%), whereas OZ-6 is dominated by *C. vidua* (65–79%). OZ-7 reveals relatively high percentages of *F. fabaeformis* (up to 18%), which appears for the first time in the upper part of OZ-5, but is absent in the upper half of OZ-6.

OZ-8 (52–21 cm, ca. 2070–800 cal yr BP) is dominated by *P. parallela*? and *C. candida* with few occurrences of *P. compressa*?, *C. vidua, F. fabaeformis* and *L. inopinata*. The uppermost OZ-9 reveals a very low absolute valve numbers represented by a few specimens of *L. inopinata, C. candida, P. compressa*?, *P. kraepelini* and *F. fabaeformis*.

4.4. Molluscs

In each of the five analysed samples only very few individuals were preserved well-enough to be identified to the species level (Fig. 9). Especially in samples from 25 to 26 cm (ca. 980 cal yr BP) and 33–34 cm (ca. 1310 cal yr BP), the gastropod and bivalve shells are broken and appear abraded and corroded. Abundant juvenile forms in the samples from 33 to 34 (ca. 1310 cal yr BP) and 229–230 cm (ca. 12,230 cal yr BP) did not allow a reliable identification or, for many specimens, identification only to genus-level. The high morphological variability of some *Gyraulus* species (see *Gyraulus crista* in Glöer, 2002, Fig. 297) further complicated a precise taxonomic identification.

The five test samples yielded 39 identifiable gastropods and 14 bivalves. Most abundant are representatives of the gastropod genus *Gyraulus* (n = 37). Additionally, there are *Valvata cristata* (O.F. Müller, 1774) (n = 1) and *Lymnaea* sp. (n = 1). The identified *Gyraulus*
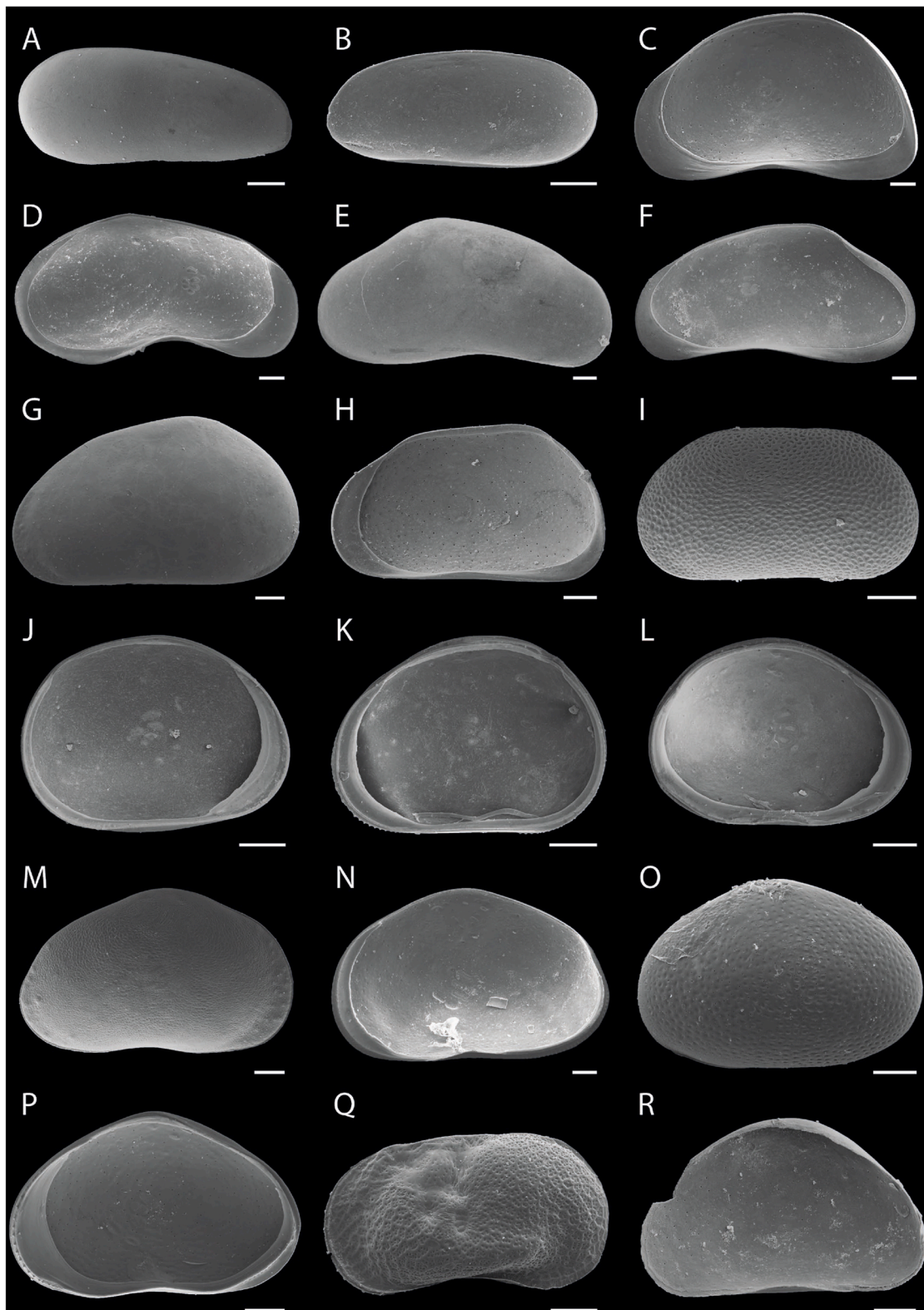
Fig. 8. Specimens of determined ostracod species extracted from sediment samples of the studied section of the Och18-II sediment core: (A–B) *Darwinula stevensoni* (Brady and Robertson, 1870), right valve: (A) external view, (B) internal view; (C) *Candona candida* (O.F. Müller 1776), right valve, internal view; (D) *Fabaeformiscandona fabaeformis* (Fischer, 1851), left valve, internal view; (E–F) *Fabaeformiscandona hyalina* (Brady and Robertson, 1870), right valve: (E) external view, (F) internal view; (G–H) *Pseudocandona compressa*? (Koch, 1838): (G) left valve, external view, (H) right valve, internal view; (I) *Pseudocandona parallela*? (G.W. Müller, 1900), left valve, external view; (J–K) *Physocypria kraepelini* (G.W. Müller, 1903): (J) left valve, internal view, (K) right valve, internal view; (L) *Cyclocypris ovum* (Jurine, 1820), left valve, internal view; (M–N) *Heterocypris salina* (Brady, 1868), right valve: (M) external view, (N) internal view; (O–P) *Cypridopsis vidua* (O.F. Müller, 1776): (O) left valve, external view, (P) right valve, internal view; (Q) *Limnocythere inopinata* (Baird, 1843), left valve, external view; (R) *Potamocypris villosa* (Jurine, 1820), right valve, internal view. Scale bars represent 100 μm.
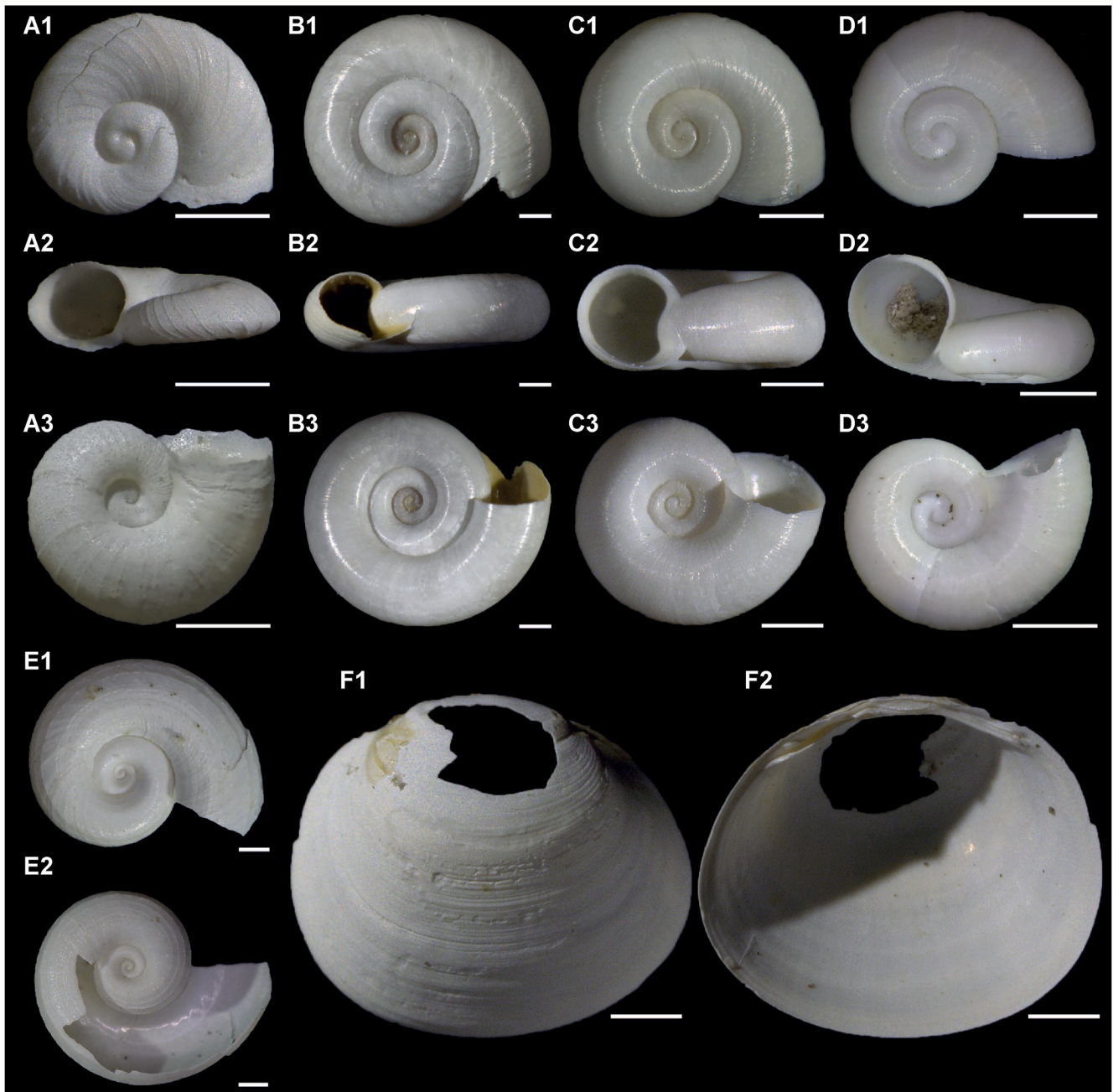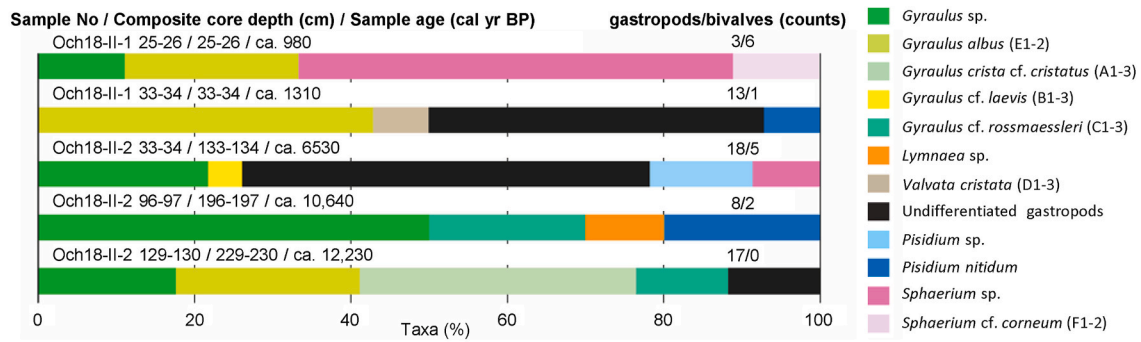
Fig. 9. Percentage diagram showing results of malacological analysis of the five selected test samples and the photographic images of the most common taxa: (A–E) gastropods in top (1), apertural (2) and umbilical (3) view; A – *Gyraulus crista* (Linnaeus, 1758); B – *Gyraulus laevis* (Alder, 1838); C – *Gyraulus rossmaessleri* (Auerswald, 1851); D – *Valvata cristata* (Müller, 1774); E – *Gyraulus albus* (Müller, 1774); (F) external and internal view of a bivalve *Sphaerium* cf. *Corneum* (Linnaeus, 1758). Scale bars represent 500 μm (A–E) and 1000 μm (F).

specimens (n = 23) comprise four species: *G. albus* (O.F. Müller, 1774) (n = 12), *G. crista* (*G. crista* cf. *Cristatus*) (n = 6), *G.* cf. *laevis* (Alder, 1838) (n = 1) and *G.* cf. *rossmaessleri* (n = 4). The bivalve fraction only contains two genera with two species, *Pisidium nitidum* (Jenyns, 1832) (n = 3) and *Sphaerium* cf. *Corneum* (Linnaeus, 1758) (n = 1). Some broken or less well-preserved bivalve shells could only be attributed to the genera *Sphaerium* sp. and *Pisidium* sp.

4.5. Zooarchaeological data

The obtained ¹⁴C dating results along with the calibrated ages of the available archaeological animal bone material from the Ochaul site are presented in Table 3. The 95% probability ranges of the calibrated ages demonstrate hunting activities and multi-phase use of the site during the Mesolithic (8851–8449 cal yr BP) and Neolithic (6837–6507; 6487–6296 and 5716–5489 cal yr BP) periods, but also during the Iron Age (2124–1930 cal yr BP). The identified bone remains suggest that roe deer, elk and possibly red deer were hunted during these intervals. One date from a bone sample of an extinct wild horse (27,785–27,158 cal yr BP, 95% probability range) indicates that the site was already visited by Upper Palaeolithic hunter-gatherers.

5. Discussion

5.1. Vegetation and climate history

5.1.1. Lateglacial (ca. 13,500–11,650 cal yr BP)

Our data suggest that the landscape around the lake was well vegetated, with AP taxa contributing ca. 50–60% to the pollen assemblage between ca. 13,500 and 12,660 cal yr BP (Fig. 10A), while herbaceous pollen contributed about 30% during that time. High percentages of birch and spruce pollen led to the reconstruction of the taiga forest as the dominant biome (Fig. 10B). However, still relatively high contributions of boreal shrubs and herbaceous taxa indicate patchy vegetation with tundra and steppe communities occupying a greater area than today. Most likely, woody vegetation mainly occupied floodplain environments with sufficient moisture supply, while drier slopes were covered with herbaceous vegetation.

A noticeable change in the pollen assemblages occurred ca. 12,660–11,680 cal yr BP, when percentages of boreal shrubs and dwarf shrubs increased up to 37.5% mainly at the expense of AP (39–45%). This change in the pollen assemblage, indicating an opening of the landscape, a spread of tundra and a reduction of boreal forest vegetation, is dated to the cold Younger Dryas oscillation (Walker et al., 2009), which followed the relatively warm Allerød interstadial. Both these millennial-scale oscillations are well recognized in annual temperature (e.g. Fig. 10E) and summer precipitation (e.g. Fig. 10I) records from the Northern Hemisphere (NH) (Nakagawa et al., 2021) and in pollen records from the Eurasian mid-latitudes (e.g. Litt et al., 2009; Bezrukova et al., 2010; Tarasov et al., 2021). The discussion on the presence/absence of trees and forest vegetation across northern Eurasia during the YD has a long history (Khotinsky, 1977; Khotinsky and Klimanov, 1997; Tarasov et al., 2009b; Kossler, 2010). Evidence of directly-dated arboreal plant macrofossils from locations as far north as the Arctic circle (e.g. Binney et al., 2009; Müller et al., 2010), leaves no doubts that patchy forests, which developed already during the Bølling–Allerød interstadial, could survive the YD and allowed quick afforestation of Eurasia within the present-day forest zone in the Early Holocene (e.g. Binney et al., 2017). This conclusion is supported by the robustly dated pollen record from Lake Ochaul (Fig. 10A), which indicates a forest-tundra landscape during the YD, suggesting that the climatic were sufficiently warm and humid. Drought-indicator taxa like *Artemisia* and Chenopodiaceae also do not show increase in pollen percentages and affinity scores of the steppe biome remain relatively low.
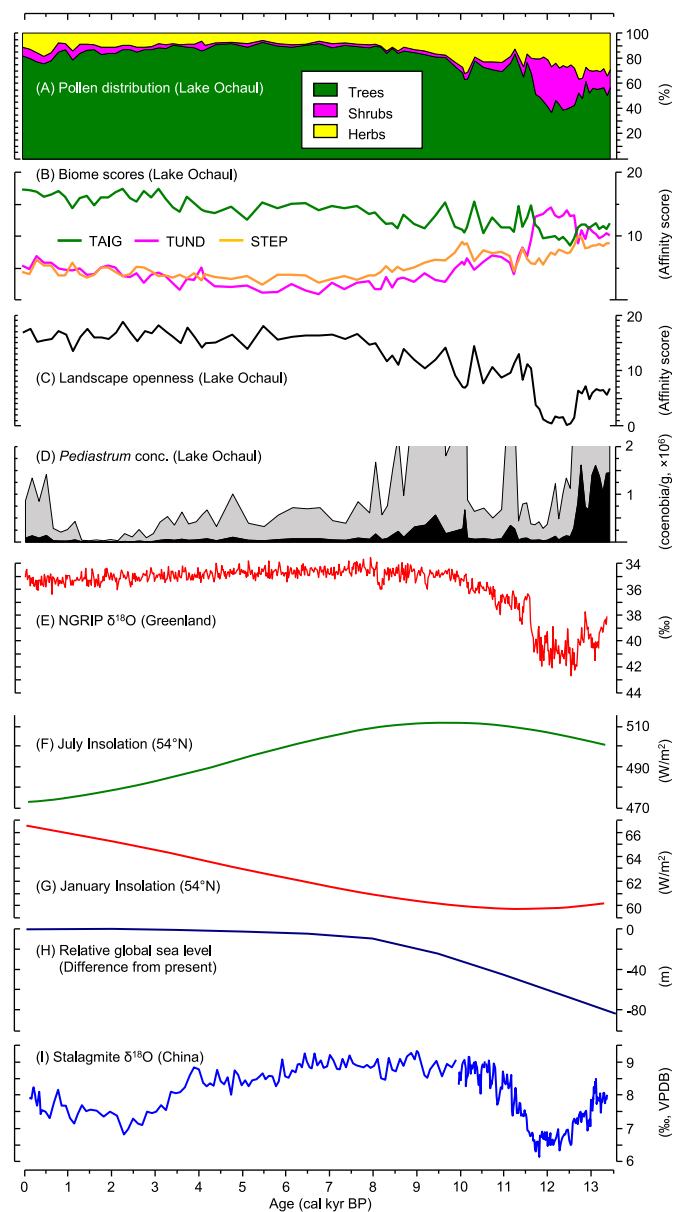

Fig. 10. Chart compilation showing (A) the pollen percentage distribution of tree, shrub and herb pollen, (B) the calculated biome scores for taiga (TAIG), tundra (TUND) and steppe (STEP), (C) the landscape openness index and (D) the *Pediastrum* algae concentrations from the Och18-II sediment core from Lake Ochaul (this study) and selected palaeoclimate data including (E) the NGRIP ice core δ¹⁸O record (after Svensson et al., 2008), the computed mean (F) July and (G) January insolation at 54°N (after Laskar et al., 2004), (H) the reconstructed changes in relative global sea level (after Waelbroeck et al., 2002) and (I) the stalagmite δ¹⁸O record D4 from Dongge cave in China (after Yuan et al., 2004).

5.1.2. Early Holocene (ca. 11,650–8000 cal yr BP)

The onset of the Holocene interglacial is marked by a strong increase in AP percentages. This and the reconstructed dominance of the taiga biome indicate a rather quick spread of boreal trees, reflecting an increase in air temperatures documented in an NH climate record from Greenland (Fig. 10E). The spread of fir, spruce and Siberian pine – boreal evergreen conifers with relatively high moisture requirements (Prentice et al., 1992, 1996) – suggests that water was not a limiting factor for tree growth during the Early Holocene between ca. 11,650 and 8000 cal yr BP. On the other hand, relatively high *Artemisia* pollen percentages and the increased scores of the steppe biome, which shifts to second place between taiga and tundra (Fig. 10B), likely indicate unstable and

periodically or seasonally dry climate. Such climate could be a result of greater-than-present continentality associated with a lower-than-present global sea level (Fig. 10H), greater-than-present difference between summer and winter insolation (Fig. 10F and G) and presence of remnants of the ice sheets in the northern parts of Europe and North America. Compared to all other sections, fern spores appear at elevated numbers. A qualitative assessment of landscape openness, calculated as the difference between the maximal forest biome score (i.e. taiga) and the maximal open biome (i.e. tundra or steppe) score (Tarasov et al., 2013), shows a trend towards a more forested landscape but suggests a lower-than-present forest coverage and greater instability in the vegetation cover during the Early Holocene interval (Fig. 10A–C). Both general trends and the short-term peaks and troughs in the arboreal pollen percentages and in the taiga biome scores match seemingly well the oxygen isotope record of NH temperature (Fig. 10E), suggesting a link between Holocene rapid climate changes (Weninger et al., 2009) and the vegetation cover (and environments) in the area of Cis-Baikal. The most striking effect was caused by the cooling episode around 11,400 cal yr BP, known in the European records as Preboreal Oscillation (PBO; Khotinsky, 1977; Björck et al., 1997; Husum and Hald, 2002). Similar to the YD oscillation, it is assumed that the cause of this cooling was a disruption of the thermohaline circulation in the North Atlantic. Unlike the YD, the PBO is seldom recognized in pollen records from northern Eurasia due to its short duration (Björck et al., 1997; Rasmussen et al., 2007). Other Early Holocene cooling events, which can be clearly traced in the Lake Ochaul pollen record include those around 10,850, 10,250 and 9200 cal yr BP. The frequently discussed event around 8200–8000 cal yr BP (e.g. Alley and Ágústsdóttir, 2005) is weakly pronounced in the pollen record (Fig. 5) by small peaks in Poaceae and *Artemisia* and a drop in the total pollen concentration.

5.1.3. Middle Holocene (ca. 8000–4200 cal yr BP)

The Middle Holocene is marked by overall stable high AP percentages and the lowest affinity scores of the tundra and steppe biomes, suggesting maximal spread of taiga forests in the region under relatively warm and moist climatic conditions that are often described as the "Holocene climate optimum". Growing pollen percentages of *Pinus sylvestris* indicate a spread of Scots pine during this time and suggest further warming of the climate and a partial degradation of permafrost, which is an important factor limiting the growth of this species in Cis-Baikal (Shumilova, 1960). Notably, the shape of the AP percentage curve (Fig. 10A) closely resembles the NGRIP isotope record (Fig. 10E), which also indicates highest mean annual temperatures and minimum variability for the entire Holocene period.

5.1.4. Late Holocene (ca. 4200 cal yr BP – present)

The transition to the Late Holocene in the Ochaul pollen record is marked by a short-term increase in shrubby birch pollen percentages between ca. 4200 and 4000 cal yr BP. This peak, indicating cooling, chronologically matches the so-called 4.2-kyear BP event, which is regarded by some researchers as one of the most severe drought events of the Holocene epoch (e.g. deMenocal, 2001; Mayewski et al., 2004; Walker et al., 2012; Roland et al., 2014; Leipe et al., 2018) and defines the beginning of the current Meghalayan age (Head, 2019). This interval is characterized by a decreasing AP percentage trend and a slow increase in the pollen percentages of small shrubs and herbaceous plants, reflected in the growing scores of the tundra and steppe biomes. Although there are no obvious changes in the reconstructed landscape openness (Fig. 10C), due to an almost parallel increase in the steppe/tundra and taiga scores, the pollen assemblage composition demonstrates higher percentages for larch and Scots pine, which usually represent more open (i.e. light taiga) forests (Alpat'ev et al., 1976). This successive cooling of the Late Holocene climate is well visible in the isotope records from Greenland and China (Fig. 10E and I) and is often associated with the weakening of the summer insolation, particularly pronounced in the NH

middle and high latitudes (Fig. 10F and G; Laskar et al., 2004; Leipe et al., 2018).

5.2. Lake system evolution

Based on the interpretation of sediment properties, geochemical analyses, as well as bioindicators the lake system evolution of Lake Ochaul is presented here. As Ti, K, Rb, Zr, and Si reflect minerogenic input to the lake (Kylander et al., 2011) and strongly correlate (Supplemental Figs. S3 and S4) – as pointed out already for the core section that covers the LGM interval (Kobe et al., 2021) – this indicates detrital clay mineral input. Although the catchment of Lake Ochaul exhibits Ca-bearing sediments and thus Ca may originate from allogenic sources, we interpret the strong positive correlation between Ca and Sr as well as the negative correlation between Ca and detrital input (K, Ti, Rb; Supplemental Fig. S4) as indication for a dominance of authigenic calcite formation within the lake. Furthermore, we interpret the strongly positive correlation between P and Ca as authigenic calcite precipitation that was mainly triggered biogenically. The geochemical and biological proxies prove limnic conditions throughout the period covered by the analysed core and anaerobic conditions near the lake floor. The latter is also suggested by the negative trend between calcite and pyrite (Supplemental Fig. S4), indicating decomposition of organic matter that decreases the pH and causes a decrease in calcite-rain to the sediment-water interface (Dean, 1990). The Ca/Ti element mole ratio mirrors detrital input with low ratios representative of increasing detrital components.

5.2.1. Lateglacial (ca. 13,500–11,650 cal yr BP)

The Lateglacial part of the Och18-II core is represented by silty clay sediment, relatively low in organic content. The lowest TOC values (ca. 5–8%) and highest Si content (ca. 15–30%) are registered in the bottommost part of the record prior to 12,800 cal yr BP. TOC increases to 10–16% and Si drops to below 10% during the YD. SiO_2bio content is very low (<0.5%) during the entire interval, in line with the very few remains of diatoms in the sediment. In contrast to diatoms, green algae *Botryococcus* and *Pediastrum* demonstrate their highest concentrations during the Allerød and an abrupt reduction during the YD, which likely reflect changes in air and water temperature.

The sedimentary elemental contents during the YD show a threefold structure of the YD with a decreasing detrital input together with increasing Ca and calcite contents between 12,660 and 12,250 cal yr BP. The following phase (ca. 12,250–12,000 cal yr BP) is marked by relatively high calcite and P contents that are accompanied by low detrital input, which is reflected by higher Ca/Ti ratios together with low values for Ti, K, Rb, Zr and Si. Thus, this phase may be interpreted to represent warmer (summer) temperatures and increased calcite formation at higher (summer) productivity. After 12,000 cal yr BP the detrital input increases again and consequently calcite and P decrease, representing a lowered productivity in the lake. Around 11,650 cal yr BP this short interval ends with the transition to the Early Holocene.

The ostracod assemblages show generally low valve numbers and species diversity. *Limnocythere inopinata* and *Heterocypris salina* are typical warm water species (Meisch, 2000; Fuhrmann, 2012). *H. salina* identified in the bottommost zone is a thermoeuryplastic species. It prefers water temperatures between 16 and 22 °C (Järvekülg, 1979) and its fossils are commonly found in interglacial and interstadial sediments (Fuhrmann, 2006, 2012). In the Lake Ochaul sediment it displays well the warm climate conditions of the Allerød interstadial.

The ostracod species identified during the YD interval are often found on phytal substrate. Even though *Candona candida* can live in a wide range of aquatic habitats (e.g. Külköylüoğlu, 2004), the species is well adapted to cold climate conditions and often found in high quantities in Lateglacial sediments (Carbonel et al., 1988; Fuhrmann et al., 1997; Meisch, 2000; Fuhrmann, 2006). The water temperature preference of *Fabaeformiscandona hyalina* is not clearly identified but it is also

often described as an oligothermophile species (Hiller, 1971). *Cypridopsis vidua* is a polythermophile species, which prefers habitats with rich aquatic vegetation (Mbahinzireki et al., 1991). For example, in assemblages from Mondsee, *C. vidua* is usually found on *Chara* stems (Danielopol et al., 1993). Furthermore, this species has a wide tolerance range to changes in pH and salinity, but a very low tolerance for poorly oxygenated waters (Külköylüoğlu, 2000). The relatively low diversity (5 species/sample) and the dominance of the oligothermophile species *C. candida* and *F. hyalina* fit well to the colder climate conditions of the YD. The high occurrences of *C. vidua* and the preferred habitat conditions of the three dominating species point to a presence of aquatic vegetation and sufficiently high oxygen contents.

The mollusc assemblage dated to the YD (ca. 12,230 cal yr BP) reveals three species of *Gyraulus*, which is the most abundant genus of gastropods in the Och18-II core. Members of this genus prefer standing or slowly flowing water and inhabit the shallow vegetated zone of a lake (Glöer, 2002, 2019; Welter-Schultes, 2012). Until recently, *G. rossmaessleri* was assumed to be only distributed in Europe (Vinarski et al., 2006). However, several studies demonstrated that this species was a member of the Siberian malacofauna during the Holocene (White et al., 2008; Makarchuk et al., 2020). *G. rossmaessleri* prefers cool waters and can be found in isolated temporary waters and ponds, swamps, wet meadows and floodplains, especially during spring (Glöer, 2002, 2019; Welter-Schultes, 2012; Antczak, 2014; Richling and Groh, 2014; Umbrecht and Bichain, 2018). On the other hand, *G. albus* found in the same sample does not tolerate the seasonal drying out of water bodies (Welter-Schultes, 2012). This and the absence of sedimentological or geochemical indications for a desiccation of Lake Ochaul during the entire YD (Kobe et al., 2021) likely indicate that *G.* cf. *rossmaessleri* specimens were transported into the deeper central part of the lake from surrounding floodplains or wet meadows. The YD sample also contains *G. crista* (*G. crista* cf. *Cristatus*?). *G. crista* prefers the vegetated littoral or even the shorelines of permanent lakes (Richardot-Coulet and Alfaro-Tejera, 1985; Glöer, 2002; Welter-Schultes, 2012; Spyra and Strzelec, 2013). Spyra and Strzelec (2013) found that the ribbed subspecies *G. crista cristatus* is especially abundant on *Typha* remains, but also on *Phragmites* and *Nuphar* debris, suggesting that the vegetated lake margin was relatively close to the Och18-II coring site.

5.2.2. Early Holocene (ca. 11,650–8000 cal yr BP)

The Holocene onset in the Och18-II core is clearly marked by a transition to organic gyttja rich in mollusc and ostracod shells, indicating a shift to warmer conditions. The Early Holocene interval reveals rather stable TIC values (7–10%) and increasing TOC values up to 16% around 10,000 cal yr BP. The geochemical record shows an increase in Ca (300 mg/g), almost negligible Si content, and lowest variability in all measured parameters. Green algae concentrations reveal a moderate increase and a greater variability, however, never reach the Allerød levels. Three distinct peaks in *Pediastrum boryanum* are registered at ca. 11,200, 10,100 and 9400 cal yr BP, however, no clear correlation between the Och18-II *Pediastrum* record (Fig. 10D) and the NH temperature (Fig. 10E) and Asian summer monsoon variability (Fig. 10I) can be established, suggesting that a complex interplay of regional and local factors and internal processes drove the Lake Ochaul system evolution.

In the ostracod assemblage, the polythermophile species *Limnocythere inopinata* (Meisch, 2000) predominates. It usually occurs in high numbers in warmer and calm waters with high sedimentation and detritus content and on a soft muddy bottom (Jungwirth, 1979). As a non-swimming, crawling species *L. inopinata* usually prefers the stagnant parts of lakes with a macrophyte debris-rich lake bottom (Meisch, 2000; Szlauer-Łukaszewska, 2008). *Darwinula stevensoni* usually inhabits the epilimnion of warm stagnant waters and as a viviparous species, it does not tolerate a complete freezing of lake bottom water (Fuhrmann, 2012). Although, *D. stevensoni* is widely distributed today, fossil occurrences of this meso-to polythermophile species (Yavuzatmaca and Külköylüoğlu, 2019) are mostly constrained to interglacial

and interstadial sediments (Fuhrmann, 2006), which further supports warmer conditions during this interval.

The Early Holocene sample dated to ca. 10,640 cal yr BP reveals the presence of the gastropod *G.* cf. *rossmaessleri* and the bivalve mollusc *Pisidium nitidum*. Species of *Pisidium* inhabit a broad range of freshwater environments (Zettler and Glöer, 2006; Welter-Schultes, 2012). Dussart (1979b) points out that the ecological requirements may vary strongly within the genus and even within the species *P. nitidum* in different geographical areas. *P. nitidum* lives in/on muddy substrate, tolerates eutrophic conditions but prefers oxygenated and clean waters (Welter-Schultes, 2012). This species occurs in vegetated lakes and in slowly flowing waters but avoids swamps and temporary water bodies as well as very cold environments (Dussart, 1979b; Zettler and Glöer, 2006; Welter-Schultes, 2012).

5.2.3. Middle Holocene (ca. 8000–4200 cal yr BP)

All analysed sediment properties and geochemical variables remain very stable during the entire Middle Holocene, suggesting a stable lake system. The TOC values vary around 8.5% and are slightly lower than during the Early Holocene. Green algae concentrations and aquatic and riparian plant taxa pollen and spore percentages are the lowest of the entire record, suggesting that the lake was at its deepest stage during this period.

In the ostracod assemblages *C. vidua* became the dominant species after 8000 cal yr BP. In contrast to *L. inopinata*, *C. vidua*, as a good swimmer, is mostly found in association with water plants and algae in more turbulent, well-oxygenated environments (Scharf, 1988, 1998; Meisch, 2000). A shift from *L. inopinata* to *C. vidua* as the prevailing species was for example observed in the littoral zone of Lake Trasimeno (central Italy), where *C. vidua* dominated the assemblages of very shallow areas with high TOC content and high abundances of macrophytes and algae (Marchegiano et al., 2017), while *L. inopinata* dominated the assemblages of slightly deeper environments. Based on these observations, the transition from *L. inopinata* to *C. vidua*-dominated assemblages in Lake Ochaul could indicate a progressive shallowing of the lake due to its filling with sediments after ca. 8000 cal yr BP. The trend of a decreasing Ca/Ti ratio and thus slightly increasing detrital input after 8000 cal yr BP may corroborate this interpretation of progressive shallowing. Another interpretation is a change in trophic conditions towards a reduction of macrophytes and algae and a slightly deeper environment at the coring site. The recorded drops in aquatic pollen percentages and in green algae concentrations ca. 8000–4000 years ago may support this interpretation. However, the occurrences of small quantities of *F. fabaeformis* ca. 6000–5000 cal yr BP indicate a rather shallow environment, as this species usually prefers shallow lake habitats (Meisch, 2000).

In one Middle Holocene sample (ca. 6530 cal yr BP), *G.* cf. *laevis* was identified along with species of the bivalve genera *Sphaerium* and *Pisidium*. All these taxa often occur in the shallow and vegetated parts of lakes with meso-to eutrophic, but well oxygenated conditions (Glöer, 2002; Welter-Schultes, 2012). *G.* cf. *laevis* is calciphile (Glöer, 2002) and indicates that the water chemistry in Lake Ochaul also favoured carbonate production as further supported by calcified charophyte remains and the green algae *Phacotus* (Supplemental Fig. S1) that are found in the Middle Holocene interval, when TIC and calcite show their highest values within the record.

5.2.4. Late Holocene (ca. 4200 cal yr BP – present)

With the onset of the Late Holocene the sediment analyses show a distinct increase in SiO_2bio content, accompanied by an increase in water content and decrease in dry bulk density, both accompanied by an increase in TOC to its highest values (up to 28.3%). The green algae concentrations remain very low, but *Myriophyllum* shows its highest pollen percentages during this interval.

A marked change in the ostracod assemblage occurred later, i.e. around 2070 cal yr BP. Since then, *P. parallela*? a taxon usually found on

muddy bottom substrate in the shallow littoral zone of small lakes (Meisch, 2000), appears in higher numbers, in comparison to the samples below.

The Late Holocene interval is represented by two samples (ca. 1310 and 980 cal yr BP) with identified mollusc remains. Among them, there are two bivalves, *S.* cf. *Corneum* and *P. nitidum*, and two gastropods, *G. albus* and *V. cristata*. *G. albus* tolerates a wide range of ecological conditions, but is usually encountered in standing or slowly flowing permanent waters. This mainly detritus feeding species lives on muddy substrates in the sublittoral of vegetated lake areas (Welter-Schultes, 2012; Antczak, 2014). It was described as an indicator for relatively clear mesotrophic and unpolluted natural waters (Glöer, 2002; Antczak, 2014), however, can tolerate highly polluted waters especially in respect to nitrogen content (Çabuk et al., 2004; Zeybek et al., 2012). The controlling factor on the abundance of *G. albus* is the presence of an organic-rich muddy substrate (Dussart, 1979a; Glöer, 2002), which is the characteristic sediment in the upper part of the Och18-II core. *V. cristata* is a calciphile species, which also occurs in the shallow and vegetated parts of lakes with meso-to eutrophic, but well-oxygenated conditions (Glöer, 2002; Welter-Schultes, 2012). The bivalve species *S.* cf. *Corneum* and *P. nitidum* prefer similar habitats, although can also populate deeper parts of a lake (Welter-Schultes, 2012; Antczak, 2014). Thus, the ecological preferences of the identified species indicate a mesotrophic shallow lake with muddy vegetated bottom substrate and relatively warm and clean water. These shallowing conditions are corroborated by the sediment analyses that show increasingly lower Ca/Ti ratios that are accompanied by higher Si (quartz and SiO_2bio), K and Rb contents. This trend accelerated from around 2200 cal yr BP and is reflected in increased pyrite, but decreased calcite, formation.

Notable for the entire Och18-II record is the absence of characteristic deep-water fauna and that all identified taxa require vegetated habitats. Light availability is one of the most important factors controlling the abundance and composition of submersed macrophyte communities that can be linked to water depth (Barko et al., 1986). *Najas* and *Potamogeton* seeds, *Ceratophyllum* debris and *Myriopyhllum* pollen were found throughout the analysed part of the core. The optimum water depth for the identified species usually does not exceed 3–4 m (Gross et al., 2003; Wersal and Madsen, 2011; Ye et al., 2018; He et al., 2019), except for *Ceratophyllum* which may also grow in deeper water (Gross et al., 2003; Ye et al., 2018). This implies that Lake Ochaul was not significantly deeper than today during the past 13,500 years.

5.3. Natural environments and traces of human activities

Along with climate change, human activities should not be neglected in the discussion of the factors which could influence changes in the pollen assemblages (e.g. Dimbleby, 1985). The area around Lake Ochaul has a very sparse population and small-scale agriculture and sedentary life style are mainly associated with settlers from European Russia, who arrived to the CIS-Baikal region in small numbers in the 17th century. However, the earliest evidence for human presence at the lake goes back to ca. 27,780–27,160 cal yr BP, based on the AMS-dated wild horse bone sample from the archaeological layers of the Ochaul site (Table 3). The pollen record from the Last Glacial Maximum section of the Och18-II sediment core reveals that NAP is, with over 90%, predominant in the pollen assemblages throughout this time interval, with the most abundant taxa being grasses (up to 51%) and sedges (7–39%), followed by Brassicaceae, Asteraceae, *Artemisia* and other minor herbaceous taxa (Kobe et al., 2021). This productive herbaceous vegetation reconstructed around the studied lake, but also for the larger region of Eastern Siberia (e.g. Bezrukova et al., 2010; Müller et al., 2010, 2014; Ashastina et al., 2018), attracted numerous large herbivores representing the Late Pleistocene mammoth fauna (Khenzykhenova et al., 2019; Kuznetsova et al., 2019) as well as their human predators (Tarasov et al., 2021). Further ^{14}C dating of the animal bone material from the Ochaul site (Table 3) indicates discontinuous hunting activities during the

Mesolithic (ca. 8850–8450 cal yr BP), Early, Middle and Late Neolithic (between ca. 6840 and 5490 cal yr BP) and the Iron Age (ca. 2120–1930 cal yr BP). Apparently, the river valley and the lake shores covered with herbaceous and aquatic vegetation and birch trees remained attractive for roe deer, elk and red deer and for Holocene hunter-gatherers, who obviously continued living in the region even during the Middle Neolithic cultural "hiatus" (ca. 6660–6060 cal yr BP) that is well-documented in the Cis-Baikal archaeological records (e.g. Weber, 2020). While the advantages of the landscapes around Lake Ochaul for prehistoric hunter-gatherers seem relatively clear, we do not know whether human activities affected the surrounding vegetation. The 95% probability ranges of the zooarchaeological dates correspond with the minor drops in the AP percentage curve; however, further detailed study on the charcoal particles in the archaeological layers may provide a better insight into the frequency of human occupations, while microcharcoal analysis of the Lake Ochaul sediment will furthermore help to reconstruct the history of forest fires in the area.

The first evidence for agricultural activities in the Ochaul pollen record (Fig. 5) can be first seen in the sample dated to ca. 2580 cal yr BP, which reveals single Cerealia and *Epilobium* pollen grains, which could be an indicator of small-scale slash-and-burn farming. While plant cultivation near the lake is unlikely, the archaeological record from Trans-Baikal demonstrates the spread of agropastoral communities in the second part of the 1st millennium BCE (Kradin et al., 2021). Pollen grains of cereal plants (including *Secale*) together with pollen of hemp appear more frequently in the uppermost pollen zone, although the low concentrations point to a far-distant origin.

6. Conclusions

This study presents a detailed and continuous fossil pollen record and quantitative biome reconstruction results from Cis-Baikal covering the last ca. 13,500 years. Major pollen composition changes in the Lake Ochaul sediments coincide with temperature changes documented in ice cores from Greenland, proving that the constructed age-depth model is accurate and the obtained pollen data are suitable for a robust reconstruction of postglacial vegetation dynamics around the lake and a discussion of the underlying climate changes.

The ratios of tree, shrub and herbaceous pollen and the biome reconstruction demonstrate that during the Allerød interstadial the region around Lake Ochaul was dominated by sparse taiga forests. During the YD, cooling led to the spread of boreal shrubs and dwarf shrubs and a more open, tundra landscape, although trees did not disappear, but formed patchy forest stands in climatically favourable environments. This facilitated a rapid spread of forests at the onset of the Early Holocene, although forest density was below modern levels until the Middle Holocene. The study region was probably characterized by seasonally dry climate, controlled by the interplay of higher insolation, lower global sea levels and remaining ice sheets in the North Atlantic region. After the Middle Holocene, during which the region saw thermal and moisture optimum conditions and a maximum spread of forests, the climate continuously cooled during the Late Holocene, paralleled by a trend towards slightly more open forest landscapes. In addition to these long-term trends, the pollen data also indicate several relatively short episodes of vegetation change, which coincide with short-term (centennial-scale) NH cooling/drying phases. This shows that the regional vegetation reacted sensitively to these climate oscillations.

The obtained ostracod and mollusc records from the core sediment were shown to be suitable for reconstructing the evolution of the Lake Ochaul aquatic system. The data show lake level changes during the last 13,500 years, but also indicate that the lake never dried out, not even during the YD. This suggests that the lake was an important source of water for herbivores and thus an important hunting ground for prehistoric hunter-gatherer groups perhaps since the Palaeolithic. As suggested by ^{14}C dates of zooarchaeological remains from the nearby archaeological site, hunter-gatherers were also present in the area

during the so-called cultural hiatus proposed for Cis-Baikal during the Middle Neolithic (ca. 6660–6060 cal yr BP). Our study highlights the great potential for future research involving systematic excavation of archaeological sites next to Lake Ochaul in combination with charcoal particle analysis of the lake sediment to gain detailed insights into human occupation and natural fire history during the Late Pleistocene–Holocene interval.

Author contributions

Conceptualisation, F.K., E.V.B., M.W., P.E.T.; Material and data collection, F.K., E.V.B., P.E.T., J.G., P.O., S.A.P., A.A.S., C.L.; Methodology, F.K., J.G., P.O., S.A.P., A.A.S., G.A.D., E.M.O., T.G.; Analysis, F.K., P.H., E.V.B., J.G., P.O., S.A.P., A.A.S., G.A.D., E.M.O., T.G.; Writing (original draft), F.K., P.E.T., C.L.; Writing (review and editing), F.K., E.V.B., M.W., P.E.T., P.H., J.G., P.O., S.A.P., A.A.S., G.A.D., E.M.O., T.G., C.L.; Visualization, F.K., P.E.T., P.H., J.G., P.O., A.A.S., C.L.

Data availability

All data used to support the findings of this study are available in the paper and its supplementary files.

Declaration of competing interest

The authors declare that they have no known competing financial interests or personal relationships that could have appeared to influence the work reported in this paper.

Acknowledgements

Appendix A. Supplementary data

Supplementary data to this article can be found online at https://doi. org/10.1016/j.quaint.2021.09.019.

References

Aksyonov, M.P., 2009. Paleolit i mezolit Verkhney Leny. Irkutsk State Technical University Press, Irkutsk (in Russian).

Allen, J.R.L., Thornley, D.M., 2004. Laser granulometry of Holocene estuarine silts: effects of hydrogen peroxide treatment. Holocene 14, 290–295.

Alley, R.B., Ágústsdóttir, A.M., 2005. The 8k event: cause and consequences of a major Holocene abrupt climate change. Quat. Sci. Rev. 24, 1123–1149.

Alpat'ev, A.M., Arkhangel'skii, A.M., Podoplelov, N.Y., Stepanov, A.Y., 1976. Fizicheskaya Geografiya SSSR (Aziatskaya Chast`). Vysshaya Shkola, Moscow (in Russian).

Andreev, A.A., Tarasov, P.E., 2013. Pollen records, postglacial: northern Asia. In: Elias, S. (Ed.), Encyclopedia of Quaternary Science. Elsevier, Amsterdam, pp. 164–172.

Andreev, A.A., Tarasov, P.E., Siegert, C., Ebel, T., Klimanov, V.A., Melles, M., Hahne, J., Shilova, G.N., Dereviagin, A.Y., Hubberten, H.-W., 2003. Vegetation and climate changes on the northern Taymyr, Russia during the Upper Pleistocene and Holocene reconstructed from pollen records. Boreas 3, 484–505.

Antczak, M., 2014. Palaeoecological significance of late glacial and Holocene molluscs. Acta Biol. 21, 5–21.

Ashastina, K., Kuzmina, S., Rudaya, N., Troeva, E., Schoch, W.H., Römermann, C., Reinecke, J., Otte, V., Savvinov, G., Wesche, K., Kienast, F., 2018. Woodlands and steppes: Pleistocene vegetation in Yakutia's most continental part recorded in the Batagay permafrost sequence. Quat. Sci. Rev. 196, 38–61.

Barko, J.W., Adams, M.S., Clesceri, N.L., 1986. Environmental factors and their consideration in the management of submersed aquatic vegetation: a review. J. Aquat. Plant Manag. 24, 1–10.

Bates, C.D., Coxon, P., Gibbard, P.L., 1978. A new method for the preparation of clay-rich sediment samples for palynological investigation. New Phytol. 81, 459–463.

BDP-Members, 2004. High-resolution sedimentary record in a new BDP-99 core from Posol'sk Bank in Lake Baikal. Russ. Geol. Geophys. 45, 149–175.

Belov, A.V., Ljamkin, V.F., Sokolova, L.P., 2002. Cartographic study of biota. Oblmashinform, Irkutsk (in Russian).

Bennett, K.D., Willis, K.J., 2001. Pollen. In: Smol, J.P., Birks, J.H.B., Last, W.M. (Eds.), Terrestrial, Algal and Siliceous Indicators, vol. 3. Kluwer Academic Publishers, Dordrecht.

Beug, H.-J., 2004. Leitfaden der Pollenbestimmung: für Mitteleuropa und angrenzende Gebiete. Pfeil, München.

Bezrukova, E.V., Mats, V.D., Letunova, P.P., Nakamura, T., Fuji, S., 1996. Holocene peat bogs in Prebaikalia as an object of paleoclimatic reconstructions. Geol. Geofiz. 37, 78–92 (in Russian, with English Abstract).

Bezrukova, E.V., Tarasov, P.E., Solovieva, N., Krivonogov, S.K., Riedel, F., 2010. Last glacial-interglacial vegetation and environmental dynamics in southern Siberia: chronology, forcing and feedbacks. Palaeogeogr. Palaeoclimatol. Palaeoecol. 296, 185–198.

Binney, H.A., Willis, K.J., Edwards, M.E., Bhagwat, S.A., Anderson, P., Andreev, A.A., Blaauw, M., Damblon, F., Haesaerts, P., Kienast, F.W., Kremenetski, K.V., Krivonogov, S.K., Lozhkin, A.V., MacDonald, G.M., Novenko, E.Y., Oksanen, P., Sapelko, T.V., Valiranta, M., Vazhenina, L., 2009. The distribution of late-Quaternary woody taxa in northern Eurasia: evidence from a new macrofossil database. Quat. Sci. Rev. 28, 2445–2464.

Binney, H., Edwards, M., Macias-Fauria, M., Lozhkin, A., Anderson, P., Kaplan, J.O., Andreev, A., Bezrukova, E., Blyakharchuk, T., Jankovska, V., Khazina, I., Krivonogov, S., Kremenetski, K., Nield, J., Novenko, E., Ryabogina, N., Solovieva, N., Willis, K., Zernitskaya, V., 2017. Vegetation of Eurasia from the last glacial maximum to present: key biogeographic patterns. Quat. Sci. Rev. 157, 80–97.

Björck, S., Rundgren, M., Ingólfsson, Ó., Funder, S., 1997. The Preboreal oscillation around the Nordic Seas: terrestrial and lacustrine responses. J. Quat. Sci. 12, 455–465.

Boyarkin, V.M., 2007. Geografiya Irkutskoi Oblasti. Publishing Hous Sarma, Irkutsk (in Russian).

Bronk Ramsey, C., 1995. Radiocarbon calibration and analysis of stratigraphy: the OxCal program. Radiocarbon 37, 425–430.

Bronstein, Z.S., 1947. Ostracoda presnykh vod. Fauna SSSR, rakoobraznye 2, 1–334 (in Russian).

Çabuk, Y., Arslan, N., Yılmaz, V., 2004. Species composition and seasonal variations of the Gastropoda in Upper Sakarya River System (Turkey) in relation to water quality. Acta Hydrochim. Hydrobiol. 32, 393–400.

Carbonel, P., Colin, J.-P., Danielopol, D.L., Löffler, H., Neustrueva, I., 1988. Paleoecology of limnic ostracodes: a review of some major topics. Palaeogeogr. Palaeoclimatol. Palaeoecol. 62, 413–461.

Danielopol, D., Handl, M., Yin, Y., 1993. Benthic ostracods in the pre-alpine deep lake Mondsee. Notes on their origin and distribution. Paper read at International symposium on ostracoda, 11.

Danukalova, G., Osipova, E., Khenzykhenova, F., Sato, T., 2015. The molluscs record: a tool for reconstruction of the Late Pleistocene (MIS 3) paleoenvironment of the Bolshoj Naryn site area (Fore-Baikal region, Eastern Siberia, Russia). Quat. Int. 355, 24–33.

Dean, W.E., 1990. The carbon cycle and biogeochemical dynamics in lake sediments. J. Paleolimnol. 21, 375–393.

deMenocal, P.B., 2001. Cultural responses to climate change during the Late Holocene. Science 292, 667–673.

Demske, D., Heumann, G., Granoszewski, W., Nita, M., Mamakowa, K., Tarasov, P.E., Oberhänsli, H., 2005. Late glacial and Holocene vegetation and regional climate variability evidenced in high-resolution pollen records from Lake Baikal. Global Planet. Change 46, 255–279.

Demske, D., Tarasov, P.E., Nakagawa, T., Suigetsu 2006 Project Members, 2013. Atlas of pollen, spores and further non-pollen palynomorphs recorded in the glacial-interglacial late Quaternary sediments of Lake Suigetsu, central Japan. Quat. Int. 290–291, 164–238.

Dimbleby, G.W., 1985. The Palynology of Archaeological Sites. Academic Press, New York.

DIN EN, 2001. Charakterisierung von Schlämmen – Bestimmung von Spurenelementen und Phosphor-Extraktionsverfahren mit Königswasser, Deutsche Fassung. Beuth Verlag, Berlin.

Dussart, G.B.J., 1979a. Life cycles and distribution of the aquatic gastropod molluscs *Bithynia tentaculata* (L.), *Gyraulus albus* (Müller), *Planorbis planorbis* (L.) and *Lymnaea peregra* (Müller) in relation to water chemistry. Hydrobiologia 67, 223–239.

Dussart, G.B.J., 1979b. *Sphaerium corneum* (L.) and *Pisidium* spp. Pfeiffer – the ecology of freshwater bivalve molluscs in relation to water chemistry. J. Molluscan Stud. 45, 19–34.

Edwards, M.E., Anderson, P.M., Brubaker, L.B., Ager, T.A., Andreev, A.A., Bigelow, N.H., Cwynar, L.C., Eisner, W.R., Harrison, S.P., Hu, F.-S., Jolly, D., Lozhkin, A.V., MacDonald, G.M., Mock, C.J., Ritchie, J.C., Sher, A.V., Spear, R.W., Yu, G., 2000. Pollen-based biomes for Beringia 18,000, 6000 and 0 ^{14}C yr bp. J. Biogeogr. 27, 521–554.

Falkner, G., Ripken, T.E.J., Falkner, M., 2002. Mollusques continentaux de France. Liste de référence annotée et Bibliographie. Collection Patrimoines Naturels 52, 1–350 in French.

Foster, W.J., Lehrmann, D.J., Yu, M., Ji, L., Martindale, R.C., 2018. Persistent environmental stress delayed the recovery of marine communities in the aftermath of the latest Permian mass extinction. Paleoceanography and Paleoclimatology 33, 338–353.

Fuhrmann, R., 2006. Die rezente Ostrakodenfauna Mitteldeutschlands (vorläufige Mitteilung). Mauritiana 19, 427–438.

Fuhrmann, R., 2012. Atlas quartärer und rezenter Ostrakoden Mitteldeutschlands. Naturkundliches Museum Mauritianum, Altenburg.

Fuhrmann, R., Schirrmeister, L., Pietrzeniuk, E., 1997. Ostrakoden und Mollusken aus den weichselspätglazialen Sedimenten des Biesenthaler Beckens (N-Brandenburg, Barnim). Z. Geol. Wiss. 25, 489–512.

Galaziy, G.I. (Ed.), 1993. Baikal Atlas. Federalnaya sluzhba geodezii i kartografii Rossii, Moscow (in Russian).

Glöer, P., 2002. Die Süsswassergastropoden Nord- und Mitteleuropas. ConchBooks, Hackenheim.

Glöer, P., 2019. The Freshwater Gastropoda of the West-Palaearctis. Vol. I. Fresh- and brackish waters except spring and subterranean snails. In: Identification Key, Anatomy, Ecology, Distribution, vol. 1. Published by the author, Hetlingen.

Grimm, E.C., 1987. CONISS: a FORTRAN 77 program for stratigraphically constrained cluster analysis by the method of incremental sum of squares. Comput. Geosci. 13, 13–35.

Grimm, E.C., 2011. Tilia 1.7.16 Software. Illinois State Museum, Research and Collection Center, Springfield, IL.

Gromig, R., Lebas, E., Savelieva, L., Pushina, Z., Fedorov, G., Brill, D., Lenz, M.M., Krastel, S., Wagner, B., Kostromina, N., Mustafin, M., Melles, M., 2021. Sedimentation history of lake Taymyr, central Russian Arctic, since the last glacial maximum. J. Quat. Sci. (in press).

Gross, E.M., Erhard, D., Iványi, E., 2003. Allelopathic activity of *Ceratophyllum demersum* L. and *Najas marina* ssp. *intermedia* (Wolfgang) Casper. Hydrobiologia 506, 583–589.

He, L., Zhu, T., Wu, Y., Li, W., Zhang, H., Zhang, X., Cao, T., Ni, L., Hilt, S., 2019. Littoral slope, water depth and alternative response strategies to light attenuation shape the distribution of submerged macrophytes in a mesotrophic lake. Front. Plant Sci. 10, 169.

Head, M.J., 2019. Formal subdivision of the Quaternary System/Period: present status and future directions. Quat. Int. 500, 32–51.

Hiller, D., 1971. Untersuchungen zur Biologie und zur Ökologie limnischer Ostracoden aus der Umgebung von Hamburg. Archiv für Hydrobiologie, Supplement-Band 40, 400–497.

Husum, K., Hald, M., 2002. Early Holocene cooling events in Malangenfjord and the adjoining shelf, north-east Norwegian Sea. Polar Res. 21, 267–274.

Jankovská, V., Komárek, J., 2000. Indicative value of *Pediastrum* and other coccal green algae in palaeoecology. Folia Geobot. 35, 59–82.

Jarochowska, E., Tonarová, P., Munnecke, A., Ferrová, L., Sklenář, J., Vodrážková, S., 2013. An acid-free method of microfossil extraction from clay-rich lithologies using the surfactant Rewoquat. Palaeontol. Electron. 16 (7T), 1–16.

Järvekülg, A., 1979. Donnaâ Fauna Vostočnoj Častu Baltijskogo Morâ. Sostav i ekologiâ raspredeleniâ Valgus, Tallin.

Jarvis, A., Reuter, H.I., Nelson, A., Guevara, E., 2008. Hole-filled SRTM for the globe Version 4, available from the CGIAR-CSI SRTM 90m Database. http://srtm.csi.cgiar.org.

Jungwirth, M., 1979. *Limnocythere inopinata* (Baird) (Cytheridae, Ostracoda): its distribution pattern and relation to the superficial sediments of Neusiedlersee. In: Löffler, H. (Ed.), Neusiedlersee: the Limnology of a Shallow Lake in Central Europe. Springer, Dordrecht, pp. 385–388.

Keatings, K.W., Holmes, J.A., Heaton, T.H., 2006. Effects of pre-treatment on ostracod valve chemistry. Chem. Geol. 235, 250–261.

Khenzykhenova, F., Lipnina, E., Danukalova, G., Shchetnikov, A., Osipova, E., Semenei, E., Tumurov, E., Lokhov, D., 2019. The area surrounding the world-famous geoarchaeological site Mal'ta (Baikal Siberia): new data on the chronology, archaeology, and fauna. Quat. Int. 509, 17–29.

Khokhutkin, I.M., Vinarski, M.V., Grebennikov, M.E., 2009. Semeystvo prudovikovyye Lymnaeidae (Gastropoda, Pulmonata, Lymnaeiformes). Part 1. In: Mollyuski Urala I Prilegayushchikh Territoriy. Goshchitsky Publishers, Yekaterinburg (in Russian).

Khotinsky, N.A., 1977. Holocene of the Northern Eurasia. Nauka, Moscow (in Russian with English Abstract).

Khotinsky, N.A., Klimanov, V.A., 1997. Allerød, Younger Dryas and early Holocene palaeoenvironmental stratigraphy. Quat. Int. 41/42, 67–70.

Kobe, F., Bezrukova, E.V., Leipe, C., Shchetnikov, A.A., Goslar, T., Wagner, M., Kostrova, S.S., Tarasov, P.E., 2020. Holocene vegetation and climate history in Baikal Siberia reconstructed from pollen records and its implications for archaeology. Archaeological Research in Asia 23, 100209.

Kobe, F., Leipe, C., Shchetnikov, A.A., Hoelzmann, P., Gliwa, J., Olschewski, P., Goslar, T., Wagner, M., Bezrukova, E.V., Tarasov, P.E., 2021. Not herbs and forbs alone: pollen-based evidence for the presence of boreal trees and shrubs in Cis-Baikal (Eastern Siberia) derived from the Last Glacial Maximum sediment of Lake Ochaul. J. Quat. Sci. (in press).

Komárek, J., Jankovská, V., 2001. Review of the green algal genus *Pediastrum*: Implication for pollenanalytical research. Bibliotheca Phycologica Band 108. J. Cramer/Gebr. Borntraeger, Stuttgart.

Kossler, A., 2010. Faunen und Floren der limnisch-telmatischen Schichtenfolge des Paddenluchs (Brandenburg, Rüdersdorf) vom ausgehenden Weichselhochglazial bis ins Holozän: Aussagen zu Paläomilieu und Klimabedingungen. Berliner paläobiologische Abhandlungen 11, 1–422.

Kozhova, O.M., Izmest'eva, L.R. (Eds.), 1998. Lake Baikal: Evolution and Biodiversity. Backhuys Publishers, Leiden.

Kradin, N.N., Khubanova, A.M., Bazarov, B.A., Miyagashev, D.A., Khubanov, V.B., Konovalov, P.B., Klementiev, A.M., Posokhov, V.F., Ventresca Miller, A.R., 2021. Iron age societies of Western Transbaikalia: reconstruction of diet and lifeways. J. Archaeol. Sci.: Report 38, 102973.

Külköylüoğlu, O., 2000. The importance of cosmopolitan and indicator species of Ostracoda (Crustacea) in Turkey based on some water parameters. In: Paper Read at the Sinop National Water Products Conference. Sinop, Turkey, 20–22 September, 2000.

Külköylüoğlu, O., 2004. On the usage of ostracods (Crustacea) as bioindicator species in different aquatic habitats in the Bolu region, Turkey. Ecol. Indicat. 4, 139–147.

Kuznetsova, T.V., Tumskoy, V.E., Schirrmeister, L., Wetterich, S., 2019. Palaeozoological characteristics of the late Neopleistocene–Holocene deposits of Bykovsky Peninsula, northern Yakutia. Zool. Zh. 98, 1268–1290.

Kylander, M.E., Ampel, L., Wohlfarth, B., Veres, D., 2011. High-resolution X-ray fluorescence core scanning analysis of Les Echets (France) sedimentary sequence: new insights from chemical proxies. J. Quat. Sci. 26, 109–117.

Laskar, J., Robutel, P., Joutel, F., Gastineau, M., Correia, A.C.M., Levrard, B., 2004. A long-term numerical solution for the insolation quantities of the Earth. Astron. Astrophys. 428, 261–285.

Leipe, C., Müller, S., Hille, K., Kato, H., Kobe, F., Schmidt, M., Seyffert, M., Spengler III, R., Wagner, M., Weber, A.W., Tarasov, P.E., 2018. Vegetation change and human impacts on Rebun Island (Northwest Pacific) over the last 6000 years. Quat. Sci. Rev. 193, 129–144.

Leipe, C., Kobe, F., Müller, S., 2019. Testing the performance of sodium polytungstate and peat sediment samples. Quat. Int. 516, 207–214.

Li, X., Liu, W., Zhang, P., An, Z., Zhang, L., 2007. Species, valve size, and pretreatment effects on δ^{18}O and δ^{13}C values of ostracod valves from Lake Qinghai, Qinghai–Tibet Plateau. Chem. Geol. 246, 124–134.

Litt, T., Schölzel, C., Kühl, N., Brauer, A., 2009. Vegetation and climate history in the Westeifel Volcanic Field (Germany) during the past 11 000 years based on annually laminated lacustrine maar sediments. Boreas 38, 679–690.

Holocene Zooarchaeology of Cis-Baikal. In: Losey, R.J., Nomokonova, T. (Eds.), 2017. Archaeology in China and East Asia, vol. 6. Nünnerich–Asmus Verlag & Media GmbH, Mainz.

Lynch, J., 1990. Provisional elemental values for eight new geochemical lake sediment and stream sediment reference materials LKSD-1, LKSD-2, LKSD-3, LKSD-4, STSD-1, STSD-2, STSD-3 and STSD-4. Geostand. Newsl. 14, 153–167.

Makarchuk, D.E., Yamskikh, G.Y., Lebedeva, N.V., Brungardt, V.O., Bochka, V.V., 2020. Late Holocene malacofauna-based paleoenvironmental reconstruction for the Bazaikha river and Tartat river valleys (Krasnoyarsk Depression, central Siberia). IOP Conference Series: Earth and Environmental Science 438, 012015.

Marchegiano, M., Gliozzi, E., Ceschin, S., Mazzini, I., Adatte, T., Mazza, R., Ariztegui, D., 2017. Ecology and distribution of living ostracod assemblages in a shallow endorheic lake: the example of Lake Trasimeno (Umbria, central Italy). J. Limnol. 76, 469–487.

Mayewski, P.A., Rohling, E.E., Stager, J.C., Karlén, W., Maasch, K.A., Meeker, L.D., Meyerson, E.A., Gasse, F., van Kreveld, S., Holmgren, K., Lee-Throp, J., Rosqvist, G., Rack, F., Staubwasser, M., Schneider, R.R., Steig, E.J., 2004. Holocene climate variability. Quat. Res. 62, 243–255.

Mäkelä, E.M., 1996. Size distinctions between *Betula* pollen types – a review. Grana International Journal 35, 248–256.

Mazepova, G.F., 1990. Rakushkovye Rachki (Ostracoda) Baikala. Akademia Nauk SSSR, Sibirskoe Otdelenie, Limnologicheskii Institut, Novosibirsk (in Russian).

Mbahinzireki, G., Uiblein, F., Winkler, H., 1991. Microhabitat selection of ostracods in relation to predation and food. Hydrobiologia 222, 115–119.

Meisch, C., 2000. Freshwater ostracoda of western and central Europe. In: Schwoerbel, J., Zwick, P. (Eds.), Süßwasserfauna von Mitteleuropa, Vol. 8, Crustacea. Spektrum Akademischer Verlag, Heidelberg.

Mikutta, R., Kleber, M., Kaiser, K., Jahn, R., 2005. Organic matter removal from soils using hydrogen peroxide, sodium hypochlorite, and disodium peroxodisulfate. Soil Sci. Soc. Am. J. 69, 120–135.

Mortlock, R.A., Froelich, P.N., 1989. A simple method for the rapid determination of biogenic opal in pelagic marine sediments. Deep Sea Research Part A. Oceanographic Research Papers 36, 1415–1426.

Müller, S., Tarasov, P.E., Andreev, A.A., Tütken, T., Gartz, S., Diekmann, B., 2010. Late Quaternary vegetation and environments in the Verkholyansk Mountains region (NE Asia) reconstructed from a 50-kyr fossil pollen record from Lake Billyakh. Quat. Sci. Rev. 29, 2071–2086.

Müller, S., Tarasov, P.E., Hoelzmann, P., Bezrukova, E.V., Kossler, A., Krivonogov, S.K., 2014. Stable vegetation and environmental conditions during the last glacial maximum: new results from Lake Kotokel (Lake Baikal region, southern Siberia, Russia). Quat. Int. 348, 14–24.

Nakagawa, T., Edouard, J.-L., de Beaulieu, J.-L., 2000. A scanning electron microscopy (SEM) study of sediments from Lake Cristol, southern French Alps, with special reference to the identification of *Pinus cembra* and other Alpine *Pinus* species based on SEM pollen morphology. Rev. Palaeobot. Palynol. 108, 1–15.

Nakagawa, T., Tarasov, P., Staff, R., Bronk Ramsey, C., Marshall, M., Schlolaut, G., Bryant, C., Brauer, A., Lamb, H., Haraguchi, T., Gotanda, K., Kitaba, I., Kitagawa, H., van der Plicht, J., Yonenobu, H., Omori, T., Yokoyama, Y., Tada, R., Yasuda, Y., Suigetsu 2006 Project Members, 2021. The spatio-temporal structure of the Lateglacial to early Holocene transition reconstructed from the pollen record of Lake Suigetsu and its precise correlation with other key global archives: implications for palaeoclimatology and archaeology. Global Planet. Change 202, 103493.

Nederlandse Fauna 2, 1998. De Nederlandse Zoetwatermollusken. Recente en fossiele weekdieren uit zoet en brak water. In: Gittenberger, E., Janssen, A.W. (Eds.), Nationaal Natuurhistorisch Museum Naturalis KNNV Uitgeverij. European Invertebrate survey, Nederland.

Peskov, S.A., 2016. Report on the Results of an Archaeological Exploration within the Borders of Ochaul OAN, Kachugsky Region with the Aim of Clarifying the Security, Historical and Cultural Value of the Culture Layers - Archive No. 3156/n. Irkutsk (in Russian).

Prentice, I.C., Cramer, W., Harrison, S.P., Leemans, R., Monserud, R.A., Solomon, A.M., 1992. Special paper: a global biome model based on plant physiology and dominance, soil properties and climate. J. Biogeogr. 19, 117–134.

Prentice, I.C., Guiot, J., Huntley, B., Jolly, D., Cheddadi, R., 1996. Reconstructing biomes from palaeoecological data: a general method and its application to European pollen data at 0 and 6 ka. Clim. Dynam. 12, 185–194.

Prokopenko, A.A., Bezrukova, E.V., Khursevich, G.K., Solotchina, E.P., Kuzmin, M.I., Tarasov, P.E., 2010. Climate in continental interior Asia during the longest interglacial of the past 500 000 years: the new MIS 11 records from Lake Baikal, SE Siberia. Clim. Past 6, 31–48.

Rasmussen, S.O., Vinther, B.M., Clausen, H.B., Andersen, K.K., 2007. Early Holocene climate oscillations recorded in three Greenland ice cores. Quat. Sci. Rev. 26, 1907–1914.

Reille, M., 1992. Pollen et Spores d'Europe et d'Afrique du Nord. Laboratoire de Botanique Historique et Palynologie. URA CNRS, Marseille, France.

Reille, M., 1995. Pollen et Spores d'Europe et d' Afrique du Nord. Supplement 1. Laboratoire de Botanique Hislorique el Palynologie. URA CNRS, Marseille, France.

Reille, M., 1998. Pollen et Spores d'Europe et d' Afrique du Nord. Supplement 2. Laboratoire de Botanique Historique et Palynologie. URA CNRS, Marseille, France.

Reimer, P.J., Austin, W.E.N., Bard, E., Bayliss, A., Blackwell, P.G., Bronk Ramsey, C., Butzin, M., Cheng, H., Edwards, R.L., Friedrich, M., Grootes, P.M., Guilderson, T.P., Hajdas, I., Heaton, T.J., Hogg, A.G., Hughen, K.A., Kromer, B., Manning, S.W., Muscheler, R., Palmer, J.G., Pearson, C., van der Plicht, J., Reimer, R.W., Richards, D.A., Scott, E.M., Southon, J.R., Turney, C.S.M., Wacker, L., Adolphi, F., Büntgen, U., Capano, M., Fahrni, S.M., Fogtmann-Schulz, A., Friedrich, R., Köhler, P., Kudsk, S., Miyake, F., Olsen, J., Reinig, F., Sakamoto, M., Sookdeo, A., Talamo, S., 2020. The IntCal20 northern Hemisphere radiocarbon age calibration curve (0–55 cal kBP). Radiocarbon 62, 725–757.

Richardot-Coulet, M., Alfaro-Tejera, L., 1985. The life cycle and ecology of the freshwater Planorbidae *Armiger crista* (L.). J. Molluscan Stud. 51, 35–51.

Richling, I., Groh, K., 2014. Entdeckung einer rezenten vitalen Population von *Gyraulus (Lamorbis) rossmaessleri* (Auerswald 1825) in Baden-Württemberg. Mitt. Dtsch. Malakozool. Ges. 90, 17–26.

Rogers, D.C., 2019. Phylum Mollusca (chapter 11). In: Rogers, D.C., Thorp, J.H. (Eds.), Thorp and Covich's Freshwater Invertebrates (Fourth Edition), vol. 4: Keys to Palaearctic Fauna. Elsevier, Amsterdam, pp. 309–355.

Roland, T.P., Caseldine, C.J., Charman, D.J., Turney, C.S.M., Amesbury, M.J., 2014. Was there a '4.2 ka event' in Great Britain and Ireland? Evidence from the peatland record. Quat. Sci. Rev. 83, 11–27.

Sanko, A.F., 2007. Chetvertichnyye presnovodnyye mollyuski Belarusi i smezhnykh regionov Rossii, Litvy, Pol'shi (Atlas-opredelitel'). Institute of Geochemistry and Geophysics, National Academy of Sciences of Belarus Press, Minsk (in Russian).

Savelieva, L.A., Raschke, E.A., Titova, D.V., 2013. Photographic Atlas of Plants and Pollen of the Lena River Delta. St-Petersburg State University, St-Petersburg (in Russian).

Scharf, B.W., 1988. Living ostracods from the nature reserve "Hördter Rheinaue" (Germany). In: Hanal, T., Ikeya, N., Ishizaki, K. (Eds.), Evolutionary Biology of Ostracoda. Devolopments in Paleontology and Stratigraphy 11. Elsevier, Kodansha, Tokyo, pp. 501–517.

Scharf, B.W., 1998. Eutrophication history of lake Arendsee (Germany). Palaeogeogr. Palaeoclimatol. Palaeoecol. 140, 85–96.

Schwanghart, W., Bernhardt, A., Stolle, A., Hoelzmann, P., Adhikari, B., Andermann, C., Tofelde, S., Merchel, S., Rugel, G., Fort, M., Korup, O., 2016. Repeated catastrophic valley infill following medieval earthquakes in the Nepal Himalaya. Science 351, 147–150.

Shchetnikov, A.A., Bezrukova, E.V., Matasova, G.G., Kazansky, A.Y., Ivanova, V.V., Danukalova, G.A., Filinov, I.A., Khenzykhenova, F.I., Osipova, E.M., Berdnikova, N. E., Berdnikov, I.M., Rogovskoi, E.O., Lipnina, E.A., Vorobyeva, G.A., 2019. Upper Paleolithic site Tuyana – a multi-proxy record of sedimentation and environmental

history during the Late Pleistocene and Holocene in the Tunka rift valley, Baikal region. Quat. Int. 534, 138–157.

Shumilova, L.V., 1960. The main features of the natural vegetation cover of Siberia and its geographical distribution. Proceedings of the Tomsk State University 148, 171–182 (in Russian).

Spyra, A., Strzelec, M., 2013. Occurrence and morphological variability of *Gyraulus crista* (Gastropoda: Pulmonata: Planorbidae) on different types of substratum in woodland ponds. Biologia 68, 679–686.

Stockmarr, J., 1971. Tablets with spores used in absolute pollen analysis. Pollen Spores 13, 614–621.

Sun, D., Bloemendal, J., Rea, D.K., Vandenberghe, J., Jiang, F., An, Z., Su, R., 2002. Grain-size distribution function of polymodal sediments in hydraulic and aeolian environments, and numerical partitioning of the sedimentary components. Sediment. Geol. 152, 263–277.

Svensson, A., Andersen, K.K., Bigler, M., Clausen, H.B., Dahl-Jensen, D., Davies, S.M., Johnsen, S.J., Muscheler, R., Parrenin, F., Rasmussen, S.O., Röthlisberger, R., Seierstad, I., Steffensen, J.P., Vinther, B.M., 2008. A 60000 year Greenland stratigraphic ice core chronology. Clim. Past 4, 47–57.

Szlauer-Łukaszewska, A., 2008. Migration of Ostracoda (Crustacea) in the flood zone of a big lowland river in the case of a rapid water rise. Natura Montenegrina 7, 325–334.

Tarasov, P.E., Webb III, T., Andreev, A.A., Afanas'eva, N.B., Berezina, N.A., Bezusko, L. G., Blyakharchuk, T.A., Bolikhovskaya, N.S., Cheddadi, R., Chernavskaya, M.M., Chernova, G.M., Dorofeyuk, N.I., Dirksen, V.G., Elina, G.A., Filimonova, L.V., Glebov, F.Z., Guiot, J., Gunova, V.S., Harrison, S.P., Jolly, D., Khomutova, V.I., Kvavadze, E.V., Osipova, I.M., Panova, N.K., Prentice, I.C., Saarse, L., Sevastyanov, D.V., Volkova, V.S., Zernitskaya, V.P., 1998. Present-day and mid-Holocene biomes reconstructed from pollen and plant macrofossil data from the former Soviet union and Mongolia. J. Biogeogr. 25, 1029–1053.

Tarasov, P., Granoszewski, W., Bezrukova, E., Brewer, S., Nita, M., Abzaeva, A., Oberhänsli, H., 2005. Quantitative reconstruction of the last interglacial vegetation and climate based on the pollen record from Lake Baikal, Russia. Clim. Dynam. 25, 625–637.

Tarasov, P.E., Bezrukova, E.V., Krivonogov, S.K., 2009a. Late Glacial and Holocene changes in vegetation cover and climate in southern Siberia derived from a 15 kyr long pollen record from Lake Kotokel. Clim. Past 5, 285–295.

Tarasov, P., Müller, S., Andreev, A., Werner, K., Diekmann, B., 2009b. Younger Dryas *Larix* in eastern Siberia: a migrant or survivor? PAGES News 17, 122–123.

Tarasov, P.E., Andreev, A.A., Anderson, P.M., Lozhkin, A.V., Leipe, C., Haltia, E., Nowaczyk, N.R., Wennrich, V., Brigham-Grette, J., Melles, M., 2013. A pollen-based biome reconstruction over the last 3.562 million years in the Far East Russian Arctic – new insights into climate–vegetation relationships at the regional scale. Clim. Past 9, 2759–2775.

Tarasov, P.E., Bezrukova, E.V., Müller, S., Kostrova, S.S., White, D., 2017. Chapter 2: climate and vegetation history. In: Losey, R.J., Nomokonova, T. (Eds.), Holocene Zooarchaeology of Cis-Baikal. Archaeology in China and East Asia 6. Nünnerich–Asmus Verlag & Media GmbH, Mainz, pp. 15–26.

Tarasov, P.E., Ilyashuk, B.P., Leipe, C., Müller, S., Plessen, B., Hoelzmann, P., Kostrova, S. S., Bezrukova, E.V., Meyer, H., 2019. Insight into the Last Glacial Maximum climate and environments of southern Siberia: a case study from the Baikal region. Boreas 48, 488–506.

Tarasov, P.E., Leipe, C., Wagner, M., 2021. Environments during the spread of anatomically modern humans across Northern Asia 50-10 cal. kyr BP: what do we know and what would we like to know? Quat. Int. 596, 155–170.

Umbrecht, K., Bichain, J.M., 2018. Redécouverte de *Gyraulus rossmaessleri* (Auerswald, 1852) (Gastropoda, Planorbidae) en Alsace (France, Bas-Rhin). Bulletin de La Société d'Histoire Naturelle et d'Ethnographie de Colmar 75, 41–48.

van Geel, B., 1978. A palaeoecological study of Holocene peat bog sections in Germany and The Netherlands, based on the analysis of pollen, spores and macro-and microscopic remains of fungi, algae, cormophytes and animals. Rev. Palaeobot. Palynol. 25, 1–120.

van Geel, B., 2002. Non-pollen palynomorphs. In: Tracking Environmental Change Using Lake Sediments. Springer, Dordrecht, pp. 99–119.

Vinarski, M.V., Karimov, A.V., Andreeva, S.I., 2006. Does *Gyraulus rossmaessleri* (Gastropoda: Planorbidae) inhabit Siberia? Malakol. Abh. (Dresden) 24, 65–76.

Vinogradov, V.I., Belenitskaya, G.A., Pokrovsky, B.G., Bujakaite, M.I., 2011. Isotopic-geochemical features of rocks of the middle-upper Cambrian verkhnyaya Lena formation in the Siberian Craton. Lithol. Miner. Resour. 46, 71–84.

Vogel, S., Märker, M., Rellini, I., Hoelzmann, P., Wulf, S., Robinson, M., Steinhübel, L., Di Maio, G., Imperatore, C., Kastenmeier, P., Liebmann, L., Esposito, D., Seiler, F., 2016. From a stratigraphic sequence to a landscape evolution model – late Pleistocene and Holocene volcanism, soil formation and land use in the shade of Mount Vesuvius (Italy). Quat. Int. 394, 155–179.

Waelbroeck, C., Labeyrie, L., Michel, E., Duplessy, J.C., McManus, J.F., Lambeck, K., Balbon, E., Labracherie, M., 2002. Sea-level and deep water temperature changes derived from benthic foraminifera isotopic records. Quat. Sci. Rev. 21, 295–305.

Walker, M., Johnsen, S., Rasmussen, S.O., Popp, T., Steffensen, J.-P., Gibbard, P., Hoek, W., Lowe, J., Andrews, J., Björck, S., Cwynar, L.C., Hughen, K., Kershaw, P., Kromer, B., Litt, T., Lowe, D.J., Nakagawa, T., Newnham, R., Schwander, J., 2009. Formal definition and dating of the GSSP (Global Stratotype Section and Point) for the base of the Holocene using the Greenland NGRIP ice core, and selected auxiliary records. J. Quat. Sci. 24, 3–17.

Walker, M.J., Berkelhammer, M., Björck, S., Cwynar, L.C., Fisher, D.A., Long, A.J., Lowe, J.J., Newnham, R.M., Rasmussen, S.O., Weiss, H., 2012. Formal subdivision of the Holocene Series/epoch: a discussion paper by a working group of INTIMATE (Integration of ice-core, marine and terrestrial records) and the Subcommission on

quaternary stratigraphy (international Commission on stratigraphy). J. Quat. Sci. 27, 649–659.

Weber, A.W., 1995. The Neolithic and early Bronze age of the lake Baikal region, Siberia. J. World PreHistory 9, 99–165.

Weber, A.W., 2020. Middle Holocene hunter–gatherers of Cis-Baikal, Eastern Siberia: Combined impacts of the boreal forest, bow-and-arrow, and fishing. Archaeological Research in Asia 24, 100222.

Weber, A.W., Link, D.W., Katzenberg, M.A., 2002. Hunter-gatherer culture change and continuity in the middle Holocene of the Cis-Baikal, Siberia. J. Anthropol. Archaeol. 21, 230–299.

Weber, A.W., Katzenberg, M.A., Schurr, T. (Eds.), 2010. Prehistoric Hunter-gatherers of the Baikal Region, Siberia: Bioarchaeological Studies of Past Lifeways. University of Pennsylvania Museum of Archaeology and Anthropology, Philadelphia.

Weber, A., Jordan, P., Kato, H., 2013. Environmental change and cultural dynamics of Holocene hunter-gatherers in Northeast Asia: Comparative analyses and research potentials in Cis-Baikal (Siberia, Russia) and Hokkaido (Japan). Quat. Int. 290–291, 3–20.

Weber, A.W., Bronk Ramsey, C., Schulting, R.J., Bazaliiskii, V.I., Goriunova, O.I., 2021. Middle Holocene hunter–gatherers of Cis-Baikal, eastern Siberia: chronology and dietary trends. Archaeological Research in Asia 25, 100234.

Welter-Schultes, F., 2012. European Non-marine Molluscs, a Guide for Species Identification. Planet Poster Editions, Göttingen.

Weninger, B., Clare, L., Rohling, E., Bar-Yosef, O., Böhner, U., Budja, M., Bundschuh, M., Feurdean, A., Gebel, H.-G., Jöris, O., Linstädter, J., Mayewski, P., Mühlenbruch, T., Reingruber, A., Rollefson, G., Schyle, D., Thissen, L., Todorova, H., Zielhofer, C., 2009. The impact of rapid climate change on prehistoric societies during the Holocene in the Eastern Mediterranean. Documenta praehistorica 36, 7–59.

Wersal, R.M., Madsen, J.D., 2011. Comparative effects of water level variations on growth characteristics of *Myriophyllum aquaticum*. Weed Res. 51, 386–393.

White, D., Preece, R.C., Shchetnikov, A.A., Parfitt, S.A., Dlussky, K.G., 2008. A Holocene molluscan succession from floodplain sediments of the upper Lena River (Lake Baikal region), Siberia. Quat. Sci. Rev. 27, 962–987.

Williams, J.W., Tarasov, P., Brewer, S., Notaro, M., 2011. Late Quaternary variations in tree cover at the northern forest-tundra ecotone. J. Geophys. Res. 116, 01017.

Wissing, F.N., Herrig, E., 1999. Arbeitstechniken der Mikropaläontologie – Eine Einführung. Enke, Stuttgart.

Yavuzatmaca, M., Külköylüoğlu, O., 2019. Fossil and recent distribution and ecology of ancient Asexual ostracod *Darwinula stevensoni* (ostracoda, Crustacea) in Turkey. J. Limnol. Freshwater Fisheries Res. 5, 47–59.

Ye, B., Chu, Z., Wu, A., Hou, Z., Wang, S., 2018. Optimum water depth ranges of dominant submersed macrophytes in a natural freshwater lake. PLoS One 13, e0193176.

Yuan, D.X., Cheng, H., Edwards, R.L., Dykoski, C.A., Kelly, M.J., Zhang, M.L., Qing, J.M., Lin, Y.S., Wang, Y.J., Wu, J.Y., Dorale, J.A., An, Z.S., Cai, Y.J., 2004. Timing, duration, and transitions of the last interglacial Asian monsoon. Science 304, 575–578.

Zeybek, M., Kalyoncu, H., Ertan, Ö.O., 2012. Species composition and distribution of Mollusca in relation to water quality. Turk. J. Fish. Aquat. Sci. 12, 719–727.

Zettler, M.L., Glöer, P., 2006. Zur Ökologie und Morphologie der Sphaeriidae der Norddeutschen Tiefebene. HELDIA 6, 1–61.

Zhadin, V.I., 1952. Mollyuski Presnykh Vod SSSR. USSR Academy of Sciences Press, Moscow–Leningrad (in Russian).

Zubkov, V.S., 2000. Neolit i bronzovyy vek verkhney Leny (istoriya issledovaniya i problemy izucheniya). In: Baykal'skaya Sibir' v drevnosti 2. Irkutsk Pedagogical University Press, Irkutsk, pp. 15–45 (in Russian).